FACULTY OF MEDICINE AND HEALTH SCIENCES

ESTABLISHING ZEBRAFISH EMBRYONIC MODELS TO INVESTIGATE PANCREATIC CANCER TREATMENT AND PARP INHIBITOR EFFICACY

Word count: 17,716

Lore Dobbelaere
Student number: 01507858

Supervisor(s): Prof. Dr. Kathleen Claes
Mentor: Jeroen Vierstraete

A dissertation submitted to Ghent University in partial fulfilment of the requirements for the degree of Master of Science in the Biomedical Sciences

Academic year: 2019 – 2020

GHENT UNIVERSITY

Preface

In the next fifty pages you will find the work I conducted in the last two years, my master thesis. To make all of this possible, I had a tremendous amount of help coming from a diversity of people whom I would like to thank first.

To start, I would like to thank Ghent University in general and more specific its Faculty of Medicine and Health Sciences to allow me to follow this education and to get a Master's degree of Sciences in Biomedical Sciences. These five years have been an incredible and educational experience for me.

I wish to show my gratitude to my promotor Prof. Dr. Kathleen Claes. She has given me the opportunity to work in her research group on a very interesting subject. She also gave me the chance to learn about the academic world. Additionally, I would like to thank every member of the Center of Medical Genetics in Ghent (CMGG) for teaching me. I had the opportunity to attend great lectures from professors and PhD students and I have learned interesting laboratory techniques from lab technicians. Some CMGG members just friendly showed me the way around the lab when I was lost.

Above all, I would like to thank my mentor, Jeroen Vierstraete, for his guidance. He showed me how to correctly produce scientific data and how to write a scientific research. He has spent an endless amount of time teaching me brilliant techniques and had unlimited patience despite my tremor. He trusted me to do experiments individually, gave me responsibilities and in particular he believed in my abilities.

I would like to show my gratefulness to my parents for giving me the opportunity to complete this education and I would like to thank especially my mother for calming me during many stressful times. Finally, my friends have always been an enormous part of my life and they have formed me into the person that I am today. I will be forever grateful to them.

Corona crisis

The Corona crisis influenced scientific research around the world. Due to measures taken by the Belgian government I was unable to continue laboratory work. Experiments were discontinued from the 16th of March on and this thesis was written with the obtained results supplemented with literature studies. Some experiments were completed, however many were started but not finished. The original goal was twofold.

To start, the optimization of the dissociation protocol of PANC-1 and Mia-Paca-2 cells was planned. Three methods were used to dissociate PANC-1 cells. In the first method, EDTA was used as dissociation compound. This resulted in low yield of cells with moderate viability. To improve the viability trypsin and TrypLE were investigated to be used as dissociation compounds. However, during optimization steps, the Corona crisis started and these experiments were prematurely terminated.

Engraftment of human cells in zebrafish larvae requires countless hours of practice. To practice, injection of HTC116 cells were used because these cells are easy to engraft. Injection with PANC-1 cells was tried a few times and conducted successfully in some larvae. The next step would have been optimization of the functional read-out and incubation of successfully injected larvae with anticancer compounds (gemcitabine and FOLFORINOX) to verify tumor response to compounds.

Culturing of the Mia-Paca-2 cell line was initialized one week before lockdown. Our goal was to engraft Mia-Paca-2 cells in zebrafish larvae and treat the engrafted larvae with gemcitabine to verify the higher sensitivity to gemcitabine in the zebrafish model. This cell line was freshly purchased and thus only had one vial that was in culture. Upon notice of the immediate lockdown measures, it was decided to freeze all cultures for long-term storage. Therefore, no experiments on this cell line could be conducted to optimize the dissociation protocol and no engraftment was performed using this cell line.

The second goal of this thesis was to create a model to establish novel PARP inhibitors (PARPi) *in vivo*. To do this, a Rad51 foci assay, an acridine orange assay and an eye size test were planned. The Rad51 foci assay was mostly completed. All five clinically available PARPi were investigated at a 400µM concentration and additionally olaparib and talazoparib were investigated at a 5µM concentration. Furthermore, a dose response was planned for all five PARPi. This, however was not completed. The dose response of rucaparib and veliparib were conducted. Due to a mistake in the staining protocol, the rucaparib slides had to be redone. The dose response of veliparib was successful but more data points are needed. For olaparib, an acridine orange staining and eye size test were done to prove cytotoxicity of the PARPi. The acridine orange staining obtained satisfactory results and the eye size test was concluded.

I regret the lab time that was taken away causing unfinished experiments. However, safety comes first at all cost.

List of abbreviations

µL	microliter
µM	micro molar
3D	3 Dimensional
ADP	Adenosinediphosphate
AMPK	AMP-activated protein kinase
AO	acridine orange
APC	Adenomatous polyposis coli
ATM	serine/threonine kinase
ATR	ataxia telangiectasia and Rad3-related protein
BER	Base Excision Repair
BRCA1	breast cancer 1
BRCA2	breast cancer 2
CA19-9	Cancer Antigen 19-9
CDKN2A	cyclin-dependent kinase inhibitor 2A
CI	Confidence interval
cm	Centimetre
CT	Computed Tomography
CtIP	retinoblastoma binding protein 8
DAPI	4′,6-diamidino-2-phenylindole
DDR	DNA damage response
DMEM	Dulbecco's Modified Eagle Medium
DNA	desoxyribonucleicacid
dpf	days post fertilization
dpi	days post injection
DSB	Double Strand Breaks
ECM	Extra Cellular Matrix
EDTA	Ethylenediaminetetraacetic acid
FAMMM	Familial Atypical Multiple Mole and Melanoma
FAP	Familial Adenomatous Polyposis
FBS	Fetal Bovine Serum
FDA	Food and Drugs Administration
FOLFIRINOX	Folonic Acid, 5-Fluorouracil, Irinotecan, Oxaliplatin
GDP	Guanosinediphosphate
GEF	Guanine nucleotide Exchange Factor
GTP	Guanosinetriphosphate
H&E	Haematoxylin and Eosin
HBOC	Hereditary Breast and Ovarian Cancer
hpf	hours post fertilization
HR	Homologous Recombination
IPMN	Intraductal Papillary Mucinous Neoplasm
KRAS	Kirsten Rat Sarcoma
LOF	Loss Of Function
MCN	Mucinous Cystic Neoplasm

mFOLFIRINOX	modified FOLFIRINOX
mL	Millilitre
MLH1	MutL homolog 1
mm	Millimetre
MSH2	MutS homolog 2
MSH6	MutS homolog 6
mTOR	mechanistic Target Of Rapamycin
Nacre	melanocyte inducing transcription factor A
NAD+	Nicotinamide-adenine-dinucleotide
NBS1	Nibrin
NHEJ	Non-Homologous End Joining
PALB2	Partner And Localizer of BRCA2
PanIN	Pancreatic Intraepithelial Neoplasia
PARP	poly (ADP-ribose) polymerase
PARPi	PARP inhibitor
PBS	Phosphate Buffered Saline
PCR	Polymerase Chain Reaction
PDAC	Pancreatic Ductal Adenocarcinoma
PDX	Patient Derived Xenograft
Penstrep	penicillin and streptomycin
PFA	paraformaldehyde
PMS2	PMS1 Homolog 2
PP	Pancreatic Polypeptide
PVS	Perivitelline space
Rad51	DNA repair protein RAD51
RNA	ribonucleic acid
RPA	DNA Replication Protein A
seDNA	single end DNA
SMAD4	Mothers against decapentaplegic homolog 4
SSB	Single Strand Break
ssDNA	single stranded DNA
STK11	serine/threonine kinase 11
TGF-β	Transforming Growth Factor-β
TGS	Tumor Suppressor Gene
TP53	Tumor Protein 53
VEC	Vascular Endothelial Cells

Table of contents

1. Summary

Pancreatic cancer is a devastating disease with a five-year survival rate below 9%. This poor prognosis is mainly due to late diagnosis, rapid progression, early metastasis, refractoriness to therapy and lack of therapeutic approaches.

To improve prognosis, personalized therapies are warranted. Such personalized therapy is usually performed by developing and testing patient derived mouse xenografts (mPDXs). However, several disadvantages do not allow the clinical use of mPDXs. We investigated if zebrafish embryonic xenografts (zPDX) could be a suitable alternative. To engraft human pancreatic cells in zebrafish embryos, we aimed to optimize the engraftment protocol. Three dissociation methods were investigated. The first method was mechanical but results were unsatisfying. The next method was enzymatic dissociation with trypsin or TrypLE. Some successful injections of PANC-1 cells into zebrafish were accomplished. We aimed to optimize functional read-outs of those xenografts. However, experiments were not finished due to the measures imposed by the Belgian government as response to tackle back the Covid-19 outbreak.

As approximately 10% of all pancreatic cancer patients have mutations in HR genes, these patients may benefit from therapy with PARP inhibitors (PARPi). New PARPi are being developed in search for better therapy with less adverse effects. Therefore, we tested if zebrafish larvae could serve as *in vivo* model. Three assays were used to evaluate this being the Rad51 foci, the acridine orange assay and an eye size test. Not all experiments were completed but results showed that indeed zebrafish can be used as *in vivo* models to establish novel PARPi.

2. Introduction

2.1 The pancreas

The pancreas is a lobulated organ of the digestive system. The pancreas is located on the posterior wall of the abdominal cavity[1] as shown in figure 1. Macroscopically, four parts can be distinguished: a head, a neck, a body and a tail. The pancreas consists of an endocrine and an exocrine part. The exocrine gland secretes pancreatic fluid into the duodenum. This pancreatic fluid contains enzymes for digestion like trypsin, lipase, protease and amylase[2]. These enzymes are inactive inside the pancreas and later activated in the duodenum to prevent damaging of the pancreas by the enzymes. The pancreas also secretes natriumbicarbonate to neutralize the gastric acid[3].

The endocrine part of the pancreas secretes hormones and is structured in units that are independently vascularized[4]. These units are called niches and consist of extracellular matrix (ECM) and islets (figure 2). The pancreatic islets represent only about 1% of the pancreatic tissue though it receives over 15% of all the blood flow to the pancreas[5]. The islet itself is an independent organ that consists of single cells like parenchymal cells, α-, β-, and δ-cells and pancreatic polypeptide (PP) cells[6]. These cells form a 3D structure that are connected to each other by vascular endothelial cells (VECs)[7]. Glucagon, insulin and somatostatin are secreted respectively by α-cells, β-cells and δ-cells. The PP- cells secrete pancreatic polypeptide[7].

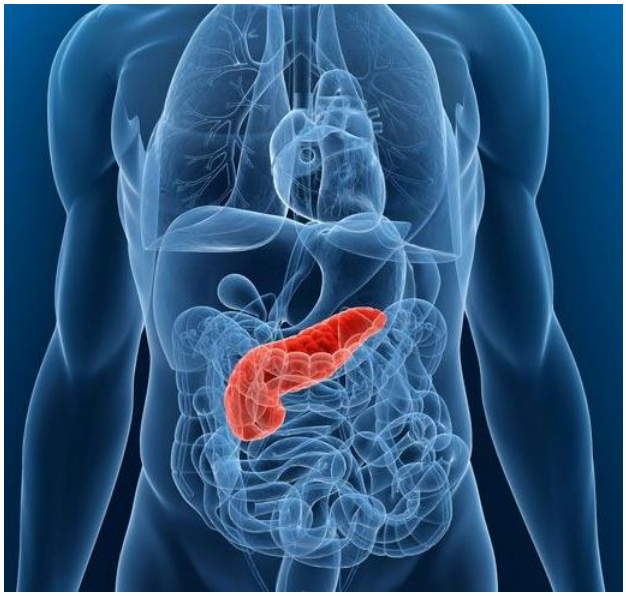

Figure 1: pancreas. Geggel et al. 2015

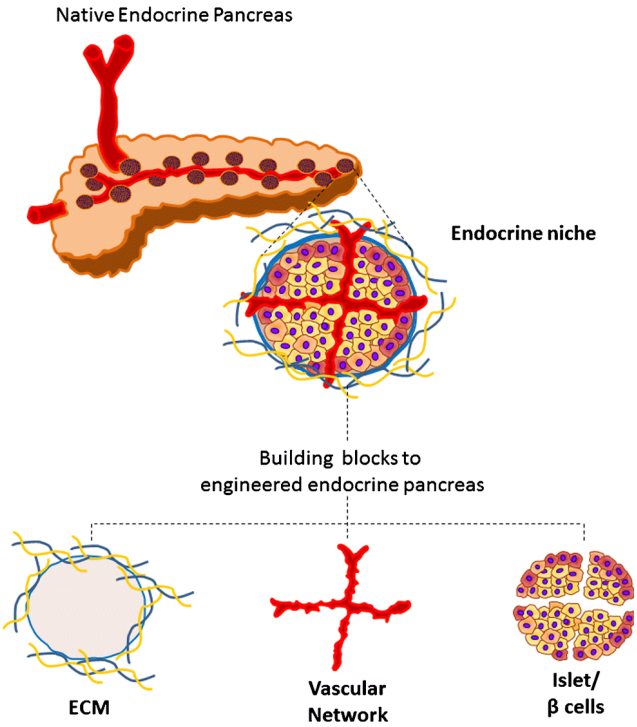

Figure 2: schematic representation of pancreatic niches. Citro et al. 2018

2.2 Pancreatic cancer

2.2.1 Incidence

Globally, pancreatic cancer is the 11th most common cancer[8]. However, it is the 7th highest cause of cancer related deaths. The incidence of pancreatic ductal adenocarcinoma (PDAC) is highest in developed countries. Europe has the highest incidence, followed by Australia, New-Zeeland and then Asia and Central America[9]. The incidence is still rising which is a major concern[10].

Pancreatic tumors are found in both the endo- and exocrine parts of the pancreas. The most common pancreatic tumor (85% of all cases) is the pancreatic ductal adenocarcinoma (PDAC) which arises in the exocrine glands. Pancreatic neuroendocrine tumors are the second most frequent tumors, but make up only about 5% of all pancreatic cancer cases[11]. Most PDAC arise in the head of the pancreas (60-70%). The rest of the tumors are found in the body (15%) and the tail (15%). However, most carcinomas have already spread to other parts of the human body upon diagnosis[12].

2.2.2 Survival rates

The 5-year survival rate for PDAC is only about 8% and most patient die within six months after diagnosis. As said before it is the seventh leading cause of cancer related deaths[8]. This poor prognosis is mainly due to late diagnosis, rapid progression, refractoriness to therapy and lack of therapeutic approaches[13].

PDAC is often diagnosed at a late stage because of non-specific symptoms. Many patients are falsely diagnosed with other diseases due to the vague symptoms[14]. Because of the relative rarity of the disease, many doctors will only see one case every few years, so awareness among doctors is of great importance to facilitate diagnosis. Metastasis is common due to the close proximity of major blood vessels[15]. These two elements (late diagnosis and early metastasis) lead to unresectable tumors in 80% of all cases[16]. Up to date, surgical removal the tumor is the only fully curative option.

2.2.3 Risk factors

There are two main subgroups of risk factors: non-modifiable and modifiable risk factors.

2.2.3.1 Non-modifiable risk factors

Non-modifiable risk factors cannot be altered by changing the life style of a person. Age is an important non-modifiable risk factor. Pancreatic cancer is most common in elderly people. 90% of all diagnoses are made in patients above the age of 55, with most patients being 70 years or older[13]. Pancreatic cancer is a multistep process. Several mutations in pancreatic cells need to occur in order for the cells to transform into malignant pancreatic cells. The older a person gets, the more chance the cells mutates in all the necessary genes[13].

Another non-modifiable risk factor is the sex[13]. More males are affected. The gap between the sexes is larger in the most developed countries. An explanation of this male predominance can be different exposure to environmental factors or alternating genetic factors between the sexes.

Ethnicity also seems to play a role. In the United States the incidence of pancreatic cancer among the African-American population is much higher than the Caucasian population[17]. The pacific

Islanders and the Asian-Americans are population groups with lower incidence rates. It is thought that the higher incidence in the African-American population is rather due to other, modifiable, risk factors like smoking, alcohol consumption and overweight, although genetic differences are also suggested[18].

Blood group is also a non-modifiable risk factor. Compared with patients that have blood group O, patients with blood group A, B or AB have significantly more risk at pancreatic cancer[19]. Gut microbiota have most likely an influence on the development of pancreatic cancer[20].

The next non-modifiable risk factor is diabetes. It is well known that patients with diabetes type I have two times more chance at developing pancreatic cancer[21]. However type II diabetes also gives an increased risk at pancreatic cancer [22].

Chronic pancreatitis is the ongoing inflammation of the pancreas. It is mainly caused by alcohol abuse and gallstones[23]. According to the results of 7 studies, patients with pancreatitis have 13 times more chance at developing pancreatic cancer than the general population[13]. The risk for pancreatitis is very divergent in different countries but overall the risk is relatively low.

Pancreatic cancer can be inheritable. A person can have germline mutations in predisposition genes of pancreatic cancer. Most of these genes are identified within multi-cancer familial syndromes[24]. Peutz-Jeghers syndrome is one such syndrome. It is an autosomal dominant disorder in which the tumors suppressor gene *STK11* is mutated. Intact *STK11* modulates many processes like energy metabolism, cell growth and apoptosis mainly through controlling the AMPK/mTOR pathway[24]. FAMMM or Familial Atypical Multiple Mole and Melanoma syndrome is known for its inactivating mutations of *CDKN2A*[24]. The normal function of CDKN2A is explained later on. Lynch syndrome is characterized by mutations in mismatch repair genes[24]. Often mutated genes are *MLH1, MSH2, MSH6* and *PMS2.* Loss of these genes creates genomic instability causing mainly colorectal tumors. Familial Adenomatous Polyposis (FAP) syndrome is also linked to an increased risk at colorectal cancer due to mutations in *APC* gene[24]. Germline mutations in *BRCA1* and *BRCA2* characterize Hereditary Breast and Ovarian Cancer (HBOC)[24]. These genes play important roles in DNA damage repair. But also *PALB2 and ATM* have been frequently found in HBOC. PALB2 is a localizer of BRCA2 and ATM plays a role in DNA repair of DNA double strand breaks. All of the aforementioned syndromes induce an increased risk at pancreatic cancer.

Cancer can also be familial. The term familial is used when two or more first degree relatives have been diagnosed with pancreatic cancer, but a clear genetic component has not been discovered[25]. People that have familial risk factors have nine times more chance at the development of pancreatic cancer in comparison with people that have no familial history. The more first degree relatives a person has, the higher the likelihood of development of pancreatic cancer[26].

2.2.3.2 Modifiable risk factors

Modifiable risk factors are elements associated with a person's lifestyle that can be adjusted in order to decrease the risk for pancreatic cancer. Important examples are cigarette smoking and alcohol abuse. Smoking of cigarettes is considered the most crucial modifiable risk factor. A study showed that there is a 74% increased risk in smokers in comparison with non-smokers[27]. Even former smokers have 20% more chance at developing pancreatic cancer. The association

between alcohol misuse and pancreatic cancer is up to date unsure[28]. There are suspicions that moderate alcohol abuse is not linked with pancreatic cancer but heavy misuse is. In addition, heavy drinking can lead to chronic pancreatitis which is a known risk factor for pancreatic cancer[29].

Obesity is a big problem in the modern world. People with obesity have an increased risk at pancreatic cancer in a way that every increase in BMI by 5 points increases the risk with 10%. It is expected that the rising incidence of pancreatic cancer is linked to the rising obesity numbers[30].

2.2.4 Pathogenesis

PDAC is a multistep process. It starts with mutations from normal mucosa to precursor lesions. The precursor lesions lead to invasive malignancy. There are three types of precursors recognized. The first one is pancreatic intraepithelial neoplasia (PanIN). This is a microscopic lesion that occurs in the small pancreatic ducts and is non-invasive. It is thought that PanIN plays a role in localized pancreatitis development. This results in an epithelial injury which may propagate into a neoplastic process[31]. It is estimated that it takes up to 11.3 years for men and 12.3 years for women to develop from PanIN to pancreatic adenocarcinoma[32].

A second precursor type is intraductal papillary mucinous neoplasm (IPMN). This is a heterogeneous group of cystic lesions[33]. The risk at malignancies is highly dependent on the ducts the lesions arose from. Malignant cells were found in 70% of the biopsies taken from the main duct in comparison with 25% in biopsies from side branches[13].

The last group is mucinous cystic neoplasm (MCN). This group accounts for a quarter of the resected pancreatic cysts[33]. They are less common than IPMN and do not involve the pancreatic duct system. They are also more common in women. 1% of all abdominal CT scans will identify a cystic lesion of the pancreas. Guidelines are needed to make sure these lesions are dealt with correctly[13].

2.2.4.1 Molecular Profile

The molecular heterogeneity of pancreatic cancer has been studied in whole exome-sequencing studies. These studies identified four common alterations: the oncogenic *KRAS* mutations and mutations of the tumor suppressor genes *CDKN2A*, *TP53* and *SMAD4*.

KRAS mutations are the first genetic alterations in the development of PDAC (figure 4). Activating KRAS mutations are found in 92% of all PDAC cases[34]. This makes it the determining factor of PDAC progression. KRAS is a member of the RAS superfamily and encodes for a GTPase that is involved in regulating processes of the cell like proliferation, differentiation, survival and migration. When the gene is intact, the KRAS protein cycles between an GTP-bound active state and a GDP-bound inactive state. The conversion from the active to the inactive state is modulated by guanine nucleotide exchange factors (GEF) and GTPase-activating proteins. GEFs catalyze exchange of GDP for GTP and GTPase-activating proteins enhance the ability of KRAS to hydrolyze GTP. This process is showed in figure 3.

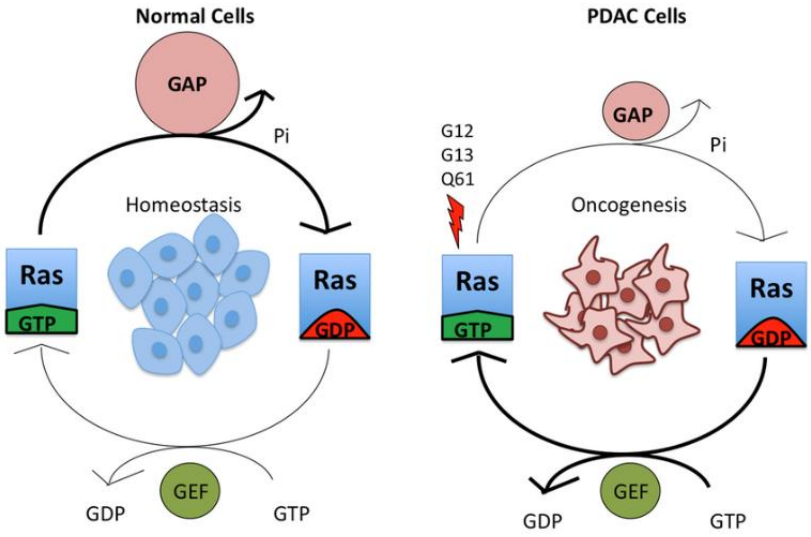

Figure 3: KRAS cycle. Zeitouni D. et al.

In a non-dividing cell KRAS is bound to GDP and thus is inactive. Growth factor stimulation causes the activation of the exchange of GDP for GTP making KRAS active. Mutations in the *KRAS* gene reduce the ability of KRAS to hydrolyze GTP making it constitutively active, hence driving tumor development. PanIN lesions are categorized into three groups of progression (I-III). PanIN lesions develop easily as an effect of *KRAS* mutations but these *KRAS* mutations are not sufficient to cause PDAC[34].

Besides the *KRAS* oncogene, mutations in several tumor suppressor genes (TSGs) are required to develop PDAC[34]. TSGs play a role in the regulation of the cell by inhibiting proliferation. TSGs can induce apoptosis, cell cycle arrest and senescence. In PDAC, *CDKN2A, TP53* and *SMAD4* are key TSGs that are frequently mutated[34]. Interestingly, the mutations occur mostly in a specific order (see figure 4).

CDKN2A encodes for a cyclin-dependent kinase inhibitor that inhibits the entry to the S-phase of the cell cycle. Most often, *CDKN2A* is the earliest TSG mutation that is seen in PDAC[34]. *CDKN2A* inactivation is often seen in slightly advanced PanIN stages prior to PDAC development. Loss of *CDKN2A* occurs directly after *KRAS* activation to inhibit the cell from going into the senescence state (see figure 4).

The second frequently mutated TSG is *TP53*. It encodes for the transcription factor p53. Loss of function (LOF) mutations are observed in a quarter of all tumors[34]. Point mutations undermine the ability of p53 to bind DNA, hence making it unable for p53 to activate factors to initiate apoptosis. Mutations in *TP53* are commonly observed in advanced PanINs after the loss of *CDKN2A* (see figure 4) although not in every pancreatic cancer case a *TP53* mutation is observed[35]. It is also thought that *TP53* mutations play an important role in the metastasis of PDAC. The function of p53 as both tumor suppressor and enhancer of metastasis shows the complexity of the molecular pathogenesis of PDAC. Inactivation of other TSGs are also seen but in lower frequency.

The role of the transforming growth factor-β (TGF-β) pathway is crucial in the development of PDAC as it can both induce apoptosis in some cases and promote invasion and metastasis in

other cases[34]. *SMAD4* is a transcriptional co-activator that regulates the anti-proliferative effect of TGF-β signaling. *SMAD4* deletions accelerate tumor development. Mutations in *SMAD4* are frequently found in advanced PanINs following *CDKN2A* mutations making *SMAD4* the last step in tumor induction (see figure 4). Loss of *SMAD4* is linked to a poor prognosis in comparison with wild type *SMAD4* expression. Recent studies are conflicting in the role of the TGF-β pathway through saying that it does not play a role in metastasis[34].

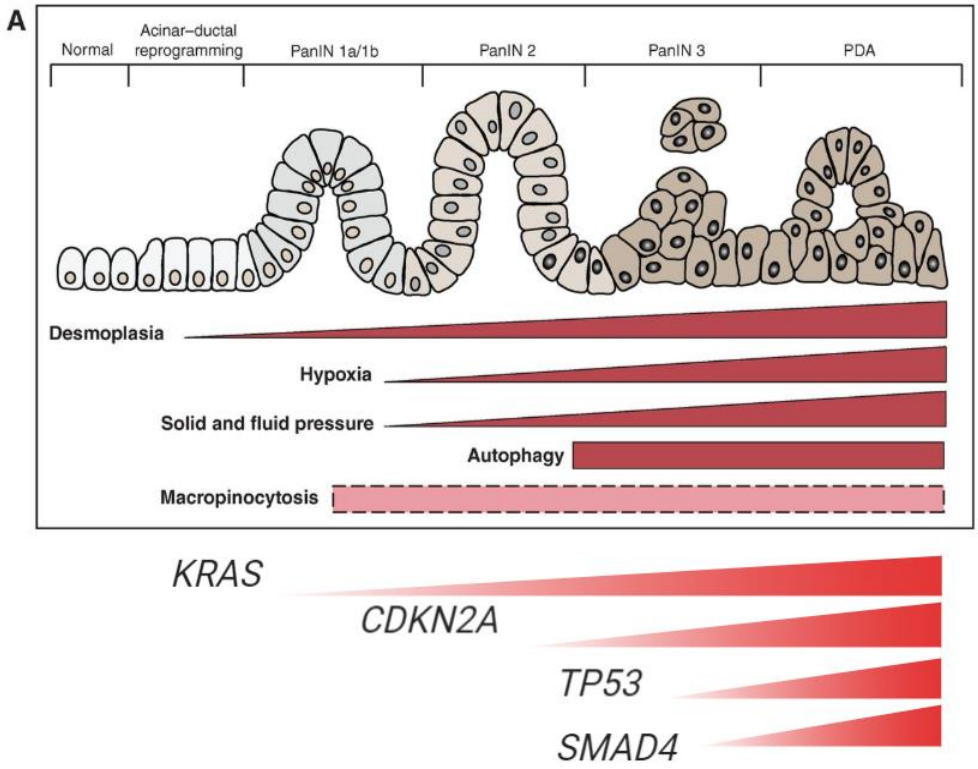

Figure 4: *schematic representation of transformation from pancreatic cell to malignant cell. Rushika, M. et al.*

2.2.4.2 Screening of PDAC

Population screenings are not recommended due to a low lifetime risk[13]. However, screening is recommended in people that match the definition of familial pancreatic cancer or patients of hereditary cancer syndromes. The low risk at developing pancreatitis together with the high risk of developing pancreatic cancer in a pancreatitis patient makes the pancreatitis population a good group for pancreatic cancer screening[13]. Intensive research including liquid biopsy is done to find potential biomarkers. Currently, serum cancer antigen 19-9 (CA19-9) is the only marker approved by the FDA in routine management of pancreatic cancer. However, this marker cannot be used as a screening biomarker due to the low positive predictive value. Patients with pancreatitis also have elevated levels of CA19-9. Its role is mainly to establish prognosis and to follow treatment response[36]. Treatment response translates in decrease of CA19-9 levels. Cell free DNA, tumor cells in circulation, volatile organic compounds in exhaled air and DNA mutations in pancreatic juice are all subjects of investigation but none of them identified a validated and specific biomarker[13]. This remains a major challenge.

2.2.5 Treatment

2.2.5.1 Surgery

As stated before, surgical resection is the only potentially fully curative option. A resectable tumor is one that has no entanglement of the superior mesenteric artery, coeliac axis, portal vein or superior mesenteric vein. A tumor is borderline resectable based on the degree of entanglement of the above mentioned structures[37]. The surgical options are distal or total pancreatectomy or pancreatico-duodenectomy (also called Whipple's surgery). The choice of the type of surgeries depends on the anatomical location of the tumor(s)[13].

Total pancreatectomy or the removal of the pancreas is difficult due to the anatomy of the pancreas. The pancreas is in contact with almost all abdominal organs. In addition, the pancreas is densely connected to the duodenum and encloses the distal common bile duct. This makes the surgery extremely complicated[38]. The surgery is represented in figure 5. The 5-year survival rate of a total pancreatectomy in PDAC patients is 18,9% according to a study by Reddy *et al.*[39]

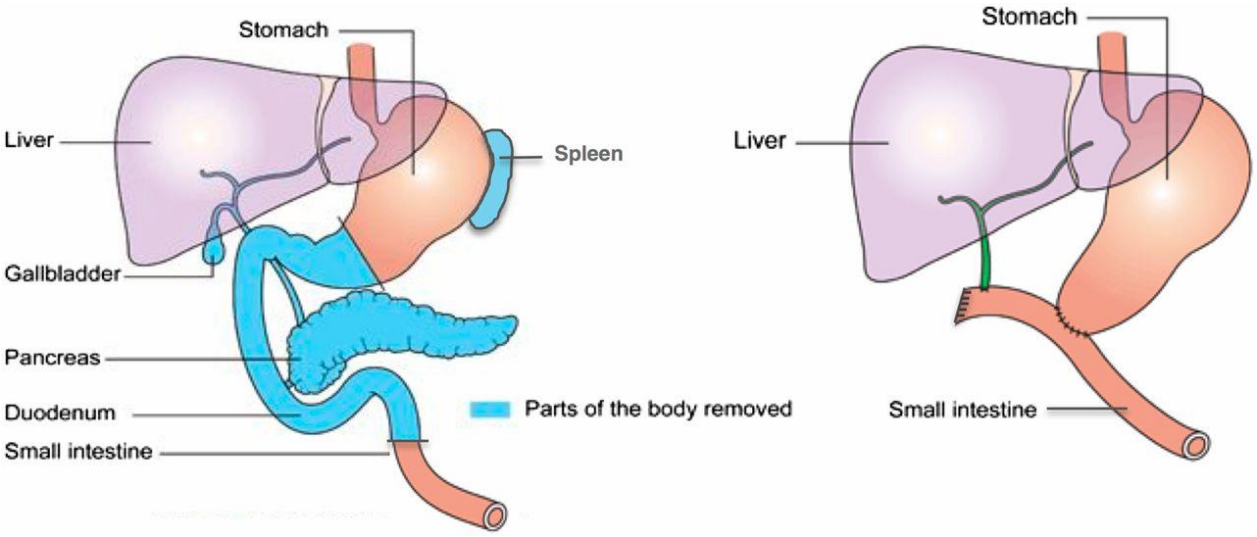

***Figure 5**: total pancreatectomy. Lund et al.*

During a Whipple's surgery, also called pancreatico-duodenectomy, the head of the pancreas, parts of the duodenum, the bile duct, the gallbladder and part of the stomach are removed. This requires outstanding surgical expertise. Figure 6 shows the modifications made during the surgery. The 5-year survival rate after a Whipple's surgery is 15-20%[40].

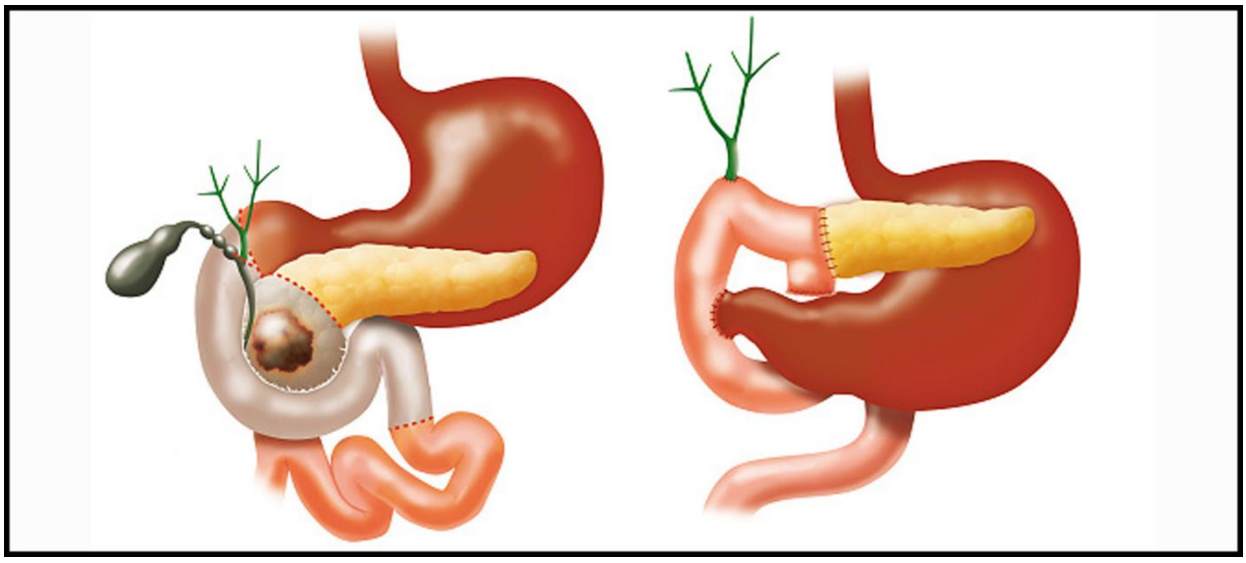

Figure 6: *Whipple's surgery*[41]

Interests in minimally invasive techniques in all areas are rising because this is correlated to less pain, shorter hospitalization time, fewer blood loss, quicker recovery, less costs and better physical appearance (cosmesis)[42]. The first minimally invasive technique is the laparoscopic distal pancreatectomy[43]. Robotic techniques to improve Whipple's surgery are investigated in several studies[44]. Results are a lower complication rate and less margin involvement. However, robotic surgery is very expensive and cost-effectiveness evaluations have yet to be made[45].

2.2.5.1 Chemotherapy

Chemoradiotherapy is cancer therapy that uses anticancer-drugs (chemotherapeutic agents) or radiation to cure cancer patients. Chemotherapy can be administered in two settings: Adjuvant and neoadjuvant therapy. Adjuvant therapy involves surgical resection of the tumor, followed by chemotherapy administration. The advised chemotherapy option has shifted over the years.

Chemoradiotherapy has long been used in locally advanced pancreatic cancer until the LAP07 study showed that there was no significant difference in overall survival with chemoradiotherapy compared to chemotherapy alone[46]. The CONKO-001 study[47] proved that administration of gemcitabine after surgery significantly increased disease free survival. Later, the ESPAC-4 study showed that dual therapy of capecitabine and gemcitabine caused better overall survival compared to gemcitabine alone[48]. Recently, the PRODIGE-24 study showed that mFOLFIRINOX treatment resulted in an improved median disease free survival compared to gemcitabine. mFOLFIRINOX is a cocktail drug that consists of modified folinic acid, 5-fluorouracil, irinotecan and oxaliplatin. However, mFOLFIRINOX was also associated with more risk at complications[49]. Because of these findings, the standard treatment choice is based on the fitness of the patient after surgery. Patients in the University Hospital in Ghent that are very fit receive adjuvant mFOLFIRINOX and the less fit patients receive gemcitabine[50].

In addition to adjuvant therapy, there is also neo-adjuvant therapy. In this kind of therapy chemotherapy is administered before surgery. Neo-adjuvant therapy attempts to eliminate micro-metastases in combination with shrinking of the primary tumor. Neo-adjuvant therapy is further

often used to treat borderline resectable tumors. The shrinking of the tumor and the elimination of micro-metastases lead to a decreased incidence of tumor recurrence[13]. In the University Hospital in Ghent patients with borderline resectable tumors receive FOLFIRINOX as neo-adjuvant therapy. There is an indication that gemcitabine plus nab-paclitaxel treatment has the same response as FOLFIRINOX but this therapy is not reimbursed in Belgium[46].

Due to late diagnosis, many patients already have metastases upon diagnosis. Control of these metastases are mainly just symptom control, management of jaundice and palliative chemotherapy[51]. Administration of FOLFIRINOX was compared to gemcitabine in palliative patients in which FOLFIRINOX showed to induce longer overall survival but again FOLFIRINOX generates more adverse effects[52]. Palliative patients in Ghent University Hopsital receive either the gemcitabine plus nab-paclitaxel treatment or FOLFIRINOX as first line chemotherapy. The second line chemotherapy is based on the first line. If the patient received gemcitabine or gemcitabine plus nab-paclitaxel as first line therapy, the second line chemotherapy will either be nonaliposomal irinotecan[53] or FOLFOX. If the patient received FOLFIRINOX as first line chemotherapy, the second line therapy will be gemcitabine.

In order to improve prognosis, more targeted therapy is under investigation. Approximately 10% of all PDAC patients have mutations in HR genes[54]. Those genes are involved in repair of DNA double strand breaks (DBS) through homologous recombination (HR). These patients may benefit from therapy with PARP inhibitors. Recently, the POLO trial showed that pancreatic cancer patients with *BRCA1/2* germline mutations have longer progression-free survival if treated with PARPi[55]. The PARPi treatment is less toxic and induces less adverse effects than the classic chemotherapies discussed above.

2.2.5.3 PARP inhibitors

Double Strand Break repair

DNA damage is a common phenomenon in human cells. DNA double strand breaks (DSBs) are especially toxic for cells, and can lead to genomic instability and ultimately tumorigenesis[56]. There are two major pathways to repair those double strand breaks: non-homologous end joining (NHEJ) and homologous recombination (HR). NHEJ is the most frequent outcome, where the DNA ends are simply re-ligated. However, this is an error-prone process. In contrast, HR uses the undamaged sister chromatid to repair the break[57]. This generates an error-free repair, but is only available in the late S-/G2- phase of the cell cycle.

Homologous recombination works as follows (figure 7). Upon a DSB, the MRE11-RAD50-NBS1 complex is recruited and bound to the break and activates the ATM kinase which initiates the DNA repair response of the cell[58]. CtIP-mediated nuclease activity leads to the formation of single stranded DNA (ssDNA). This ssDNA can be coated with DNA replication protein A (RPA) which activates ATR and facilitates the HR response. RAD51 is then localized to the ssDNA by the BRCA1-PALP2-BRCA2 complex[59], replaces the RPA complex and searches for the homologous sequence on the sister chromatid.

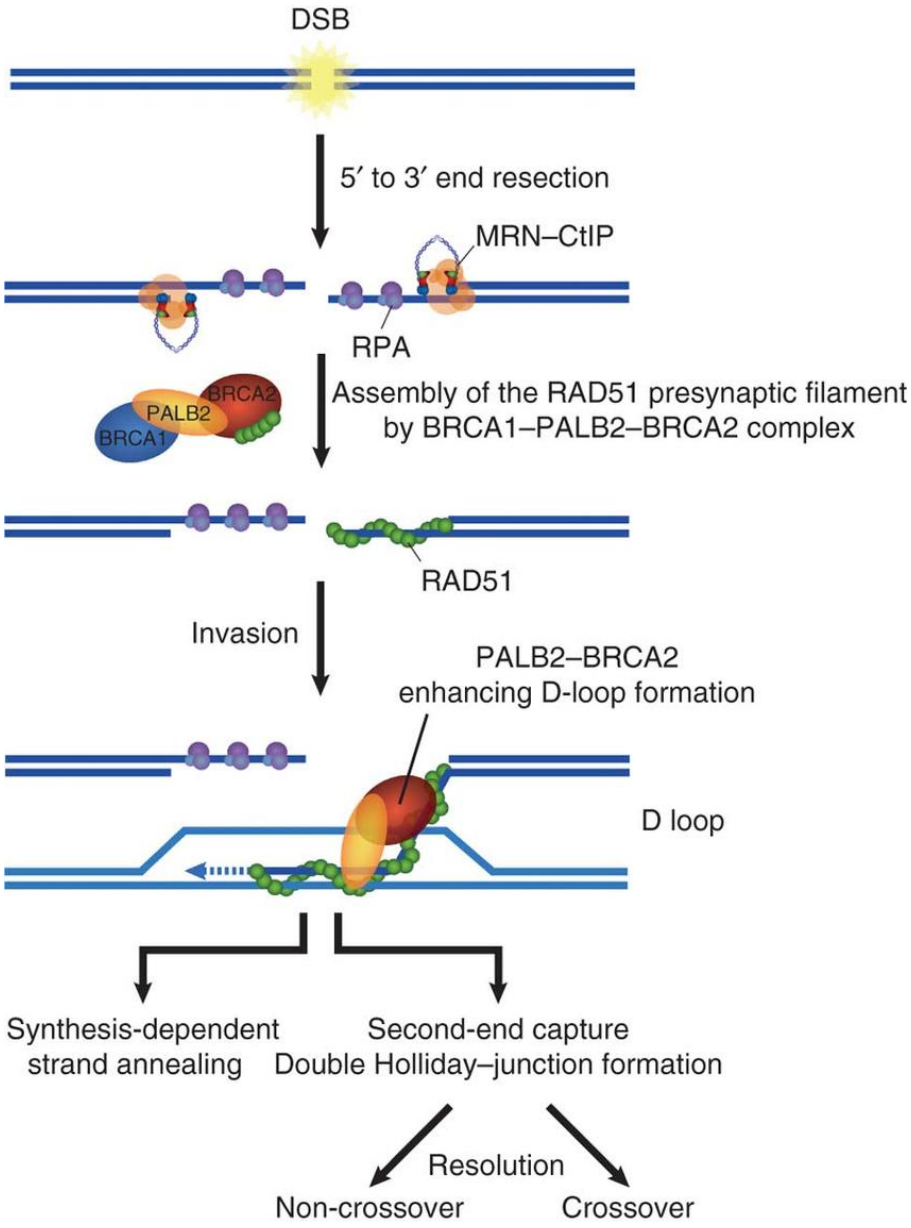

Figure 7: HR pathway by Buisson et al.[59]

<u>How does PARP inhibition cause DSB</u>

PARP or poly (ADP-ribose) polymerase is a group of proteins essential in DNA damage repair. PARP1 is of importance in the repair of single strand breaks (SSB) through base excision repair (BER). PARP inhibitors (PARPi) will inhibit the function of PARP by trapping and/or hinder the catalytic functionality. The unrepaired SSB causes replication fork stalling which induces a DSB. Normally, a DSB has two DNA ends but when a DSB is formed through replication fork stalling, there is only one DNA end. This is called single end DNA (seDNA). Normally, this break is repaired through the HR pathway but when the HR pathways is impaired this break is repaired by NHEJ which is error-prone and causes cell death[60]. This prevents the single strand break from being repaired correctly.

Synthetic lethality and PARPi

Synthetic lethality is the phenomenon where a deficiency in two genes leads to cell death, but deficiency in only one of those genes does not[61]. This approach is interesting in cancers with patients carrying germline mutations in DDR genes. As tumors deriving from these patients are often resulting from a second hit mutation, therapies that utilize the synthetic lethality approach could selectively target the tumor, while leaving normal tissue unharmed.

For PARPi, this is the case in tumors with a *BRCA1/2* mutation causing disfunction of the HR pathway. PARPi treatment causes cell death in *BRCA1/2* mutated cells due to excessive DNA damage. This phenomenon is showed schematically in figure 8. Cells with one or two functional *BRCA1/2* allele(s) will survive[62], however, when both alleles are mutated, the cell goes into apoptosis due to excessive DNA damage.

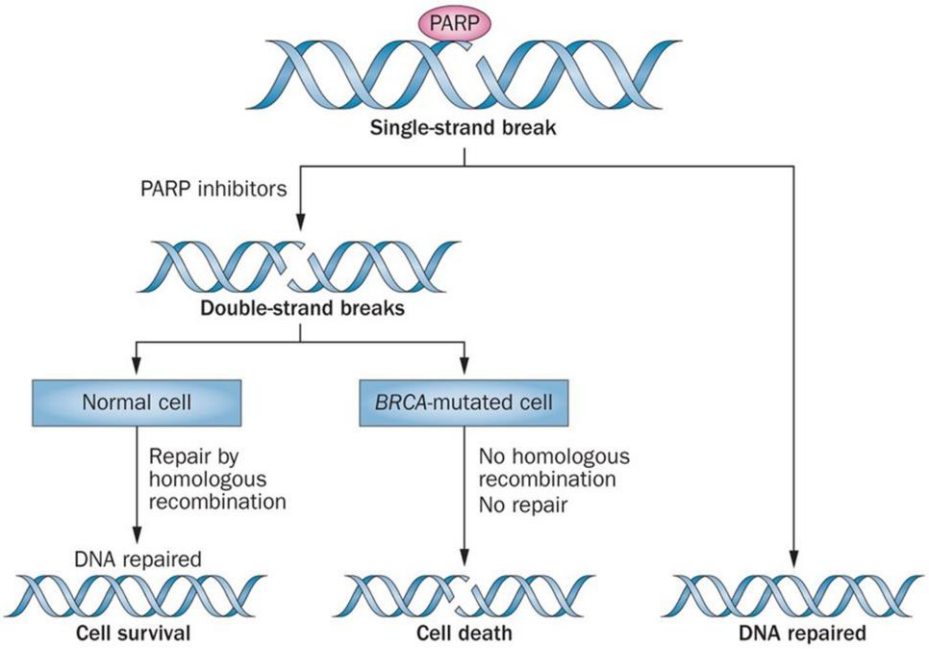

Figure 8: *synthetic lethality caused by PARPi by A. Sonnenblick. et al.[62]*

Different PARPi

Up to date there are five clinically available PARPi, being olaparib, niraparib, rucaparib, veliparib and talazoparib. PARPi work by trapping PARP onto damaged DNA and inhibiting the catalytic cavity of PARP. Some PARPi are more potent to trap and others are more potent to inhibit.

Olaparib is the best known PARPi and is reimbursed for the treatment of recurrent ovarian cancer. Olaparib is developed to inhibit the NAD^+ activity in the catalytic cavity of PARP1 and PARP2[63,64]. It is clinically proven that olaparib also benefits patients with metastatic breast or prostate cancer with germline *BRCA* mutations. A clinical trial of phase III was conducted in metastatic pancreatic cancer patients with germline mutations in *BRCA1* or *BRCA2*[55]. The overall survival of the patients

receiving olaparib is longer than those in the placebo group, nonetheless, more adverse effects were observed in the olaparib group.

Niraparib is a known maintenance treatment in recurrent ovarian cancer. Niraparib is targeted against PARP1 and PARP2. It inhibits the enzymatic activity which causes to form more PARP-DNA complexes inducing more DNA damage leading to cell death and apoptosis[65]. Clinical approval was granted after the phase III NOVA trial which proved that it was stated that the niraparib group had longer progression free-survival[65]. However these effects were regardless of the presence of *BRCA m*utations. Up to date, niraparib is not used in the clinic to treat pancreatic cancer. There are three clinical trials currently recruiting pancreatic patients in the United States that will test niraparib in pancreatic cancer patients as maintenance treatment (NCT03553004, NCT03601923, NCT03404960).

Rucaparib inhibits PARP-1, 2 and 3 by trapping these PARPs[64]. Rucaparib is approved as a treatment for ovarian cancer with *BRCA*-mutations and as maintenance therapy for recurrent ovarian cancer[66]. The phase III ARIEL3 trial showed longer progression-free-survival in the rucaparib group compared to the placebo group. Currently, there are no phase III trials ongoing for maintenance rucaparib treatment in pancreatic cancer patients.

Veliparib inhibits the catalytic activity of PARP[64]. The trapping efficacy of veliparib is much lower in comparison with olaparib, rucaparib and niraparib[67]. Veliparib was shown to have a moderate effect as anticancer therapy in prostate cancer. It is clinically used in combination treatment[68]. Currently there are no phase III trials ongoing of veliparib treatment in ovarian cancer patients but phase II trials are promising[67].

The fifth clinically available PARPi is talazoparib. Talazoparib is thought to be the most potent PARP trapper up to date[67]. The efficacy of talazoparib in ovarian cancer is still under investigation. Talazoparib has a larger structure and is more rigid than the other PARPi. The rigidity is thought to be the cause of the higher potency[67]. This PARPi also showed better progression free survival in comparison with a standard single agent therapy like capecitabine, eribulin, gemcitabine, or vinorelbine[69].

Adverse effect observed in PARPi treatment

Despite the less severe toxic effects of the PARPi in comparison with the classic chemotherapy, there are still adverse effects observed. The most common adverse events are nausea, anemia, thrombocytopenia, hypertension, sepsis and fatigue[64,65,67]. The anemia and thrombocytopenia are caused by inhibition of the HR pathway in rapidly divining cells that result in more mutations and more apoptosis of these cells. Because of these adverse effects, there is a constant search for new PARPi with fewer adverse effects.

Developing novel PARPi

New PARPi are being developed in the search of better therapy with less adverse effects. PARPi development is mainly performed using several *in vitro* assays[70]. Only in late stages of development, *in vivo* testing of PARPi is done with mouse xenografts. However these mouse xenografts are expensive and are highly time consuming. Thus, failure at this stage of development would be very unfortunate. Therefore, there is a high interest in developing alternatives of *in vivo* models that are less expensive, take less time and can be used earlier in development of a PARPi.

Zebrafish

Zebrafish or *Danio rerio* is a tropical fish that is member of the teleostei infraclass and is estimated to be arisen 340 million years ago from its common ancestor[71]. This ancestor underwent an additional genome duplication in comparison with other vertebrates causing zebrafish to have 4 copies of each chromosome. These duplications are called ohnologues[71]. Zebrafish have their origin in Southeast Asia. An adult fish is about two and a half centimeters to four centimeters long. Zebrafish models are often used in genetic studies, but also in toxicological studies, environmental health studies, metabolic diseases and so on. Zebrafish are widespread used for studying the function of vertebrate genes[71]. The Welcome Trust Sanger Institute initiated the Zebrafish genome-sequencing project in 2001. This led to insights in orthologues between the human and zebrafish genome. 71,4% of all human genes have at least one orthologue in zebrafish[71]. Reciprocally, 69% of all zebrafish genes have an orthologue in the human genome. 47% of these human orthologues have a one-to-one relationship with the zebrafish orthologue.

Advantages of zebrafish are high fecundity, rapid development, feasible manipulation due to *ex utero* development, small size and easy manipulation. Zebrafish are aquatic models that can easily take up small molecules if added to the medium[72] making compound administration effortless.

Zebrafish as a solution to early *in vivo* PARPi testing

A zebrafish model could be an answer to the problems of the PARPi development. Zebrafish are much cheaper than mice. It is relatively easy to manipulate the zebrafish genome by for example making an overexpression or a gene knockdown. It is already known that several repair pathways are conserved between zebrafish and human[73]. The HR pathway is one of them. There are several techniques available to study gene pathways in zebrafish[74].

Assays to study HR and cell death in zebrafish

Visualization of the HR pathway can be done as shown by Vierstraete *et al.*[74] Rad51 binds to Brca2 when the HR pathway is activated as discussed above. Rad51 can be visualized with immunohistochemical staining[74]. In this assay two antibodies are used to visualize the Rad51 foci. The primary antibody binds Rad51 and the second antibody is fluorescently labeled and binds the primary antibody making the Rad51 foci visible. This assay is visualized in figure 9.

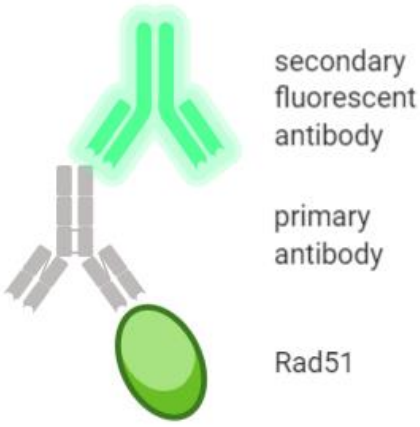

Figure 9: *immunohistochemical staining*

The acridine orange (AO) staining is a technique that can be used to identify cells in apoptosis. Acridine orange is a permeable nucleic acid dye that is closed off in different compartments like lysosomes. These compartments cannot enter the nucleus of the cell. However, when a cell is going into apoptosis, the pH in the cell changes and the acridine orange is released from the lysosomes in the cytoplasm. Once in the cytoplasm the acridine orange can localize to the nucleus and intercalate with partially uncoiled DNA. This process makes the acridine orange highly fluorescent which can be visualized and quantified easily[75].

2.2.6 Using zebrafish to model pancreatic Xenografts

Due to the low survival rates and especially the short time of survival after diagnosis, the prognosis of PDAC is very poor. Nowadays, the choice of treatment is mainly based on the condition of the patient. In order to improve the prognosis, more personal therapy approaches are needed. Up to date it is unpredictable to assess which patient will respond to which treatment. With PARPi being more and more interesting, it would be favorable to predict the response to a PARPi and other chemotherapy.

2.2.6.1 Patient derived xenografts

An option for predicting the response to the therapy of a PDAC patient is by transplanting a piece of the primary tumor of the patient into an immune compromised mouse[76]. This technique is called a patient derived xenograft (PDX). PDXs are used for drug development but also for predicting the outcome of a therapy for a patient.

However, this approach has multiple downsides. For starters, the time upon engraftment in a mouse can take up to several months, this is time the patient does not have. Additionally, the immune system of the mice would reject the human tumor tissue, therefore an immunocompromised strain is required for mice xenografts increasing the costs of the study[76]. Because of these increased costs, fewer therapies can be tested.

2.2.6.2 Zebrafish xenografts

A solution to these problems can be found in using zebrafish xenografts (zPDX). Firstly, xenografts engraft much faster in zebrafish in comparison with the time of engraftment needed in mice (days instead of months)[77]. Secondly, less tumor material is needed for engraftment, which makes that, with the same amount of material harvested from a patient, more zebrafish can be engrafted causing the ability to implement more biological replicates favoring the statistics[78]. Only about 50 to 100 cells per larvae need to be injected for successful engraftment. It has already been proven that human cells can be engrafted in zebrafish embryos[78]. Finally, zebrafish have no adaptive immune system in the embryonic stage making the use of an immunocompromised strain unnecessary which reduces the cost. The reduced costs enable to inject more embryos and thus gaining more xenografts to test multiple therapies. Other advantages are stated above (high fecundity, rapid development, feasible manipulation due to *ex utero* development, small size and easy manipulation and effortless compound administration). The Casper strain is a strain of zebrafish that lacks pigment and thus is transparent throughout their whole life[79]. This makes visualization of the xenotransplanted tissue easier.

Fior *et al*. proved that diverse behaviors of cancer cells could be measured *in vivo* only 4 days after developing a PDX model of colorectal cancer cells in zebrafish larvae[80]. When they compared

zebrafish xenografts to mouse xenografts, they observed similar sensitivities to chemotherapy. They also used the zebrafish xenografts to test the response to treatment in patients and found correlations between patients relapse time and zebrafish xenograft response to treatment. Because of the promising results of this research group, we want to test if this model can also be used for predicting treatment outcome in PDAC patients.

3. Objectives

The goal of this master thesis is twofold. The first goal is to establish and optimize a zebrafish xenograft protocol to engraft pancreatic cancer cells and assess their sensitivity to different compounds. For this optimization work, we will attempt to engraft two pancreatic cancer cell lines, PANC-1 and Mia-Paca-2. Upon establishing proper engraftment, we will treat these xenografts with the chemotherapeutic compound gemcitabine, to which Mia-Paca-2 is exceptionally sensitive. Our aim is to use our functional-readouts to observe an increased tumor response of the Mia-Paca-2 cell line to the treatment, compared to less sensitive PANC-1 cells. These optimizations will eventually lead to a zebrafish platform where we aim to predict the response to treatment in pancreatic cancer patients. In the long run, we want to engraft primary tumor material into zebrafish larvae. Subsequent to successful engraftment, compounds (gemcitabine and FOLFIRINOX) will be added to the medium of the larvae. The response to therapy in zebrafish should be similar to the response to treatment in the patient. This will ultimately lead to a platform in which a prediction can be made about which chemotherapy the patient will respond to.

The second aim is development of a zebrafish model for *in vivo* establishment of new PARPi. Mutations in the HR pathway confer an increased risk of breast, ovarian, prostate and pancreatic cancer. PARPi target tumor cells with deficiencies in the HR pathway. It is well-known that ~10% of all pancreatic cancer patients have mutations in HR genes and thus could benefit from a PARPi treatment. There is a constant search of novel PARPi with higher potency and less adverse effects. Establishment of those PARPi nowadays is mainly done *in vitro* followed by mouse xenografts late in development. To improve and fasten development of new compounds there is need for an assay that foresees *in vivo* data early in development process, provides fast results and all of that at an affordable cost. A zebrafish could accomplish the needs. Using several techniques, we will check the efficacy of all five clinically available PARPi.

4. Materials and methods

4.1 Zebrafish embryonic xenografts

4.1.1 Optimization on cell lines

4.1.1.1 Maintenance of cell lines

We aimed to inject two cell lines to engraft in zebrafish larvae. The PANC-1 cell line and the Mia-Paca-2 cell line. All cells were cultured in a humidified incubator at 37°C and 5% CO_2. The PANC-1 cell line is a human pancreatic cancer cell line. The medium used is Dulbecco's Modified Eagle Medium (DMEM) enriched with 10% fetal bovine serum (FBS) and antibiotics being 1% penicillin and streptomycin (penstrep). The Mia-Paca-2 cell line is another human pancreatic cancer cell line that should be more sensitive to gemcitabine. These cells were maintained in DMEM enriched with 10% FBS and 2,5% horse serum and 1% penstrep. The use of these cell lines was approved by the local Ethical Committee (code EC 107-2018/mf).

4.1.1.2 Labeling cells

The human pancreatic cancer cells need to be labeled with a fluorescent dye (DiI) for later visualization. DiI is a fluorescent lipophilic cationic dye from Thermo Fisher Scientific (catalogue number: V22888). Upon labeling, cells need to be dissociated in order to collect them. In this thesis, three approaches were conducted in order to find the most optimal dissociation method for pancreatic cancer cells.

EDTA

The protocol that was followed is manufactured by Fior *et al.*[80] Cells should be at 70% confluence for the right balance between optimal cell density and dividing cells. Medium was removed and cells were washed with 3 mL PBS 1x. After that PBS 1x was removed. DiI was diluted 1:1000 in PBS and 2mL was added to the cells. Cells were incubated for 10 minutes at 37°C followed by an incubation on ice for 15 minutes. During this procedure, cells are covered with aluminum foil to avoid fading of fluorescent signal. Afterwards, DiI is removed and cells were washed again with 3 mL PBS 1x. Subsequently, cells were harvested using EDTA. EDTA is a Ca^{2+} chelator that will remove the Ca^{2+} ions. Integrins needs these Ca^{2+} ions to maintain cell adhesion[81]. 2mL of EDTA was added to the cells and this was incubated for 3 minutes at 37°C. A cell scraper was used to detach the cells from the surface of the flask. The suspension containing the cells was transferred into 1,5mL Eppendorfs. In order to remove dead cells and debris, the Eppendorfs were centrifuged for 4 minutes at 300rcf at 4°C. Two pellets were formed during the centrifugation of the Eppendorfs. The pellet on the side of the Eppendorf contained dead cells and debris and needed to be removed. The lower pellet contained the vital cells. The excess fluid together with the upper pellet was removed and the lower pellet was resuspended in 60µL medium. The cells were counted and the viability is measured.

In order to quantify cell density and calculate viability, samples of cell suspension were diluted 1:10 in trypan blue. Viable cells have intact cell membrane and do not stain with trypan blue. Dead cells however have permeable membranes which allows the dye to enter and stain the cells. The cells were counted using a Burker count chamber. This chamber consist of 9 large squares ($1mm^2$). Each square is subdivided into 16 smaller squares with double lines (0,05 mm apart). These double lines form $0,0025mm^2$ squares. The depth of the square is $0,1mm^2$ making the volume in the chamber 1µL. The larger square have triple lines. When counting cells, only cells

inside the 16 squares and those that touch the upper or left triple lines were counted as showed in Figure 10. Cells outside of the larger square or those touching the bottom or right triple lines were not counted. Using this dilution, every counted cell resembles 1 million cells per mL. Three of those large squares are counted and average of those three results will be taken as end result.

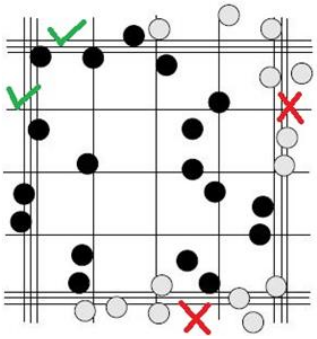

Figure 10: *Method of counting cells in Burker count chamber*

Trypsin

The previous protocol was adjusted to obtain higher viability of the cells. Washing and incubating with DiI was done as described above. Subsequently, cells were incubated for 3-7 minutes with 2mL trypsin (Life Technologies Europe, Thermo Fisher Scientific catalogue number: 25300-054). Trypsin is an enzyme which degrades proteins by cutting peptide bindings between lysine and arginine. This dissociates the cells from each other and from the surface so scraping of the cells was unnecessary. The cells are harvested and centrifuged as described above. An extra step was added to inhibit the trypsin. After removing the excess fluid cells were resuspended in DMEM to inhibit trypsin and prevent it from being toxic to the cells because incubation of the cells with trypsin for too long will damage the membrane and kill the cells. After a second centrifugation the cells were counted as described above.

TrypLE

In order to obtain even higher viability and retain more cell surface proteins, a third condition was investigated to dissociate cells. Again, the cells are washed and stained as described above. For harvesting the cells, TrypLE (Thermo Fisher Scientific, catalogue number 12605010) was used. This is a mixture of three enzymes and is thought to be less aggressive then trypsin. Washing the cells was done with PBS 1x as described above. 2mL of TrypLE was added to the cells and incubated for 3-7 minutes at room temperature. Without scraping, the cells are transferred to 1,5mL Eppendorfs and centrifuged as described above. After removal of the remnant, 60µL of cold PBS 1x was added. The cells were counted and the viability was measured as described above.

4.1.2 Injecting larvae

4.1.2.1 Maintenance of zebrafish strain

All zebrafish lines were housed in a Zebtec semi-closed recirculation housing system at a constant temperature (27°C-28°C), pH (~7,5), conductivity (~550µS) and light/day cycle (14/10). Fish were fed twice a day with dry food (Gemma Micro, Skretting) and once with artemia (Ocean Nutrition). The Casper strain is used for engrafting the cells. This strain has mutations in two genes (*rov* and *nacre*) and lacks pigment throughout their whole life making visualization of the tumor after

engraftment easier[82]. All experiments were approved by the local animal ethics committee, application number ECD 18/75.

4.1.2.2 Injection

48 hours post fertilization (hpf) larvae were injected with labeled human pancreatic cells. In this stage, most of the larvae were still in their chorion. The chorion was removed using the pronase, a mixture of enzymes that digest proteins to single amino acids[83]. The larvae were sedated with tricaine after which they could be positioned on an agar plate with lanes. The head was positioned upwards and the back of the larvae was positioned against an agar lane. An example of the positioning is showed in figure 11.

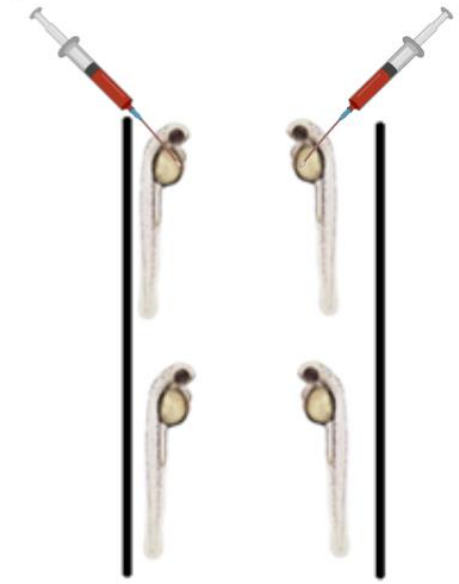

***Figure 11**: positioning larvae on agar plates. The head is positioned upwards and the back is positioned against the agar lane. Black lines are indicate lanes.*

After positioning, the larvae could be injected with the labeled cells. For injection, needles were made by pulling a borosilicate into two pieces with a TW100-4 World precision instruments with heat at 400-600, fil: 4, Vel: 46-60, Del: 200 and pull: 100. The remaining halves have a tip of approximately 1cm. This allows for shortening of the needle if obstructions occur. The optimal location for injection was in the perivitelline space (PVS) indicated in figure 12. The ideal amount of injection is described as approximately the size of an eye.

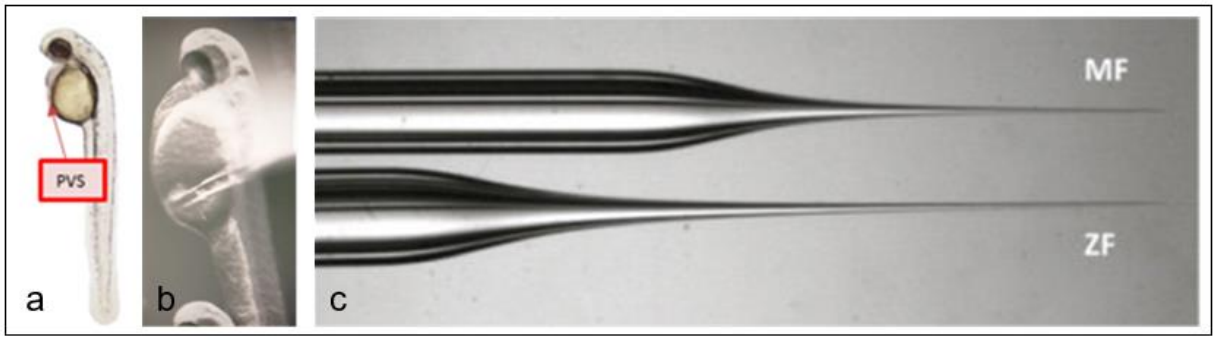

***Figure 12:** injection side and needle; **a** shows the PVS schematically in a zebrafish larvae; **b** shows an injection into the PVS; **c** displays a needle used for injection.*

After injection, the larvae were kept sedated another ten minutes to allow them to recover and prevent them from twitching and pushing out freshly injected cells. Then, larvae were transferred back into E3 medium and held in an incubator at 34°C. This temperature is a compromise between the optimal temperature for a zebrafish and the optimal temperature for human cells being 28°C and 37°C respectively[84]. Screening was done 24 hours post injection (hpi). In this screening, the viability of the zebrafish was checked together with the viability of the injected tumor cells. Larvae that were wrongly injected, had too few injected cells or appeared unacceptable were discarded.

4.1.2.3 Hematoxylin and eosin staining

After successful injection, the zebrafish could be stained with a hematoxylin and eosin (H&E) staining. This is a standard technique that is often used by pathologists to screen for cancer cells in a biopsy. Hematoxylin stains the basophilic structures purple, such as DNA and RNA. Eosin, on the other hand, stains the acidophilic structures in several shades of red. This will mostly be the cytoplasm and its structures. To do a H&E staining, the fish are euthanized with tricaine and fixed overnight in paraformaldehyde (PFA) 4%.

The next day, the fish can be dehydrated by incubating in a series of alcohol solution going from 30% ethanol, to 50%, 70%, 96% and iso-propanol (considered as 100% ethanol). The next incubation is in an iso-propanol/toluene mixture before incubation in toluene. The fish are then dehydrated and can be embedded in paraffin. After incubation at 55°C in paraffin overnight, the fish can be positioned and cut into 5µm sections. The H&E staining itself is performed in the Microm HMS 740 (protocol in addendum 1).

4.2 PARPi

4.2.1 Maintenance of the zebrafish strains

For the experiments with the PARPi the brca2^{cmg35} zebrafish strain and the *Tg(EF1a: mCherry-zGem)*^{oki011} zebrafish line were used. The housing of the strains is outlined above.

4.2.2 Treatment of PARPi

The five PARPi that were investigated were olaparib (Selleckhem: S1060), niraparib (Absource Diagnostics: S2741), rucaparib (Selleckhem: S1098), veliparib (Enzo Life Sciences: ALX-270-444-M005) and talazoparib (Bioconnect: S7048).

4.2.2.1 DMSO toxicity

As PARPi are often dissolved in DMSO, DMSO was used as negative control in the Rad51 assay, acridine orange assay and in the eye size test. However DMSO or dimethylsulfoxide itself has a certain toxicity. To check the toxicity of DMSO, an experiment was set up in which wild type larvae at 72hpf were exposed for seven hours to a concentration of DMSO ranging from 1% to 5%. For each concentration six larvae were incubated. After incubation, larvae were checked for possible malformations and viability.

4.2.2.2 Rad51 foci

Breeding

To measure the amount of Rad51 foci (marker for HR), an immune fluorescent staining was performed. For the Rad51 foci experiment, the *Tg(EF1a: mCherry-zGem)*^{oki011} strain was used.

This is a transgenic line that expresses geminin with a fluorescent tag at the amino-terminal region to visualize the cell cycle. Geminin is a DNA replication inhibitor that is present in high levels in S- and G2- phase cells. At 24hpf, larvae were screened for the presence of a geminin signal. All larvae without the fluorescent tag were discarded.

Incubation
At 3 days post fertilization (dpf), the larvae were incubated with PARPi. Fish were kept in 2mL E3 medium enriched with the desired amount of PARPi for 7 hours. For all five PARPi we incubated fish with a concentration range of PARPi between 5µM and 800µM.

Embedding
After incubation, the zebrafish were euthanized using tricaine followed by fixation for 1 hour using PFA 4%. The next day, fish were dehydrated and embedded in paraffin as described above. Sections of 5µm of the region that encloses the intestinal tract were made. In this region many dividing cells are present thus many cells in the S-/G2- phase of the cell cycle[74].

Immunofluorescent staining
To stain the larvae, anti-mCherry (visualizing Geminin; 1:1000; Abcam; ab125096) and anti-Rad51 (1:2000; Santa Cruz; H-92) were used. The secondary antibodies involved Goat-anti-rabbit Dylight 488 antibody (1:1000 Sigma-Aldrich) and Goat-anti-mouse Dylight 594 antibody (1:1000 Sigma-Aldrich). The slides were counterstained with DAPI+fluoromount (Sigma-Aldrich).

Counting foci
After staining, the slides were scanned on a Zeiss Axio Observer.Z1 inverted microscope using the Zen pro 2012 software. A 100x magnification was used and Z-stacks (0.22 µm thickness) were made for each section. The number of Rad51 foci was measured in geminin positive cells only, as only these cells are capable of performing HR.

4.2.2.3 Acridine orange assay
The larvae used for the acridine orange assay were offspring of brca2$^{cmg35/+}$ heterozygotes. Larvae 6hpf were assembled and treated with olaparib for 24 hours at a concentration of 5µM. At 32hpf, larvae were dechorionated and incubated for 15 minutes in acridine orange (AO) solution. Afterwards, the embryos were washed three times with E3 medium and sedated with tricaine.

For imaging, the embryos were positioned laterally on methylcellulose droplets. Images were taken with a Nikon SMZ18 stereoscope (FGP; 3.2x magnification, 800ms integration). ImageJ was used to select areas of the body and by using “process – find maximum” the number of apoptotic cells could be quantified (noise tolerance being 5). A normalization was preformed to correct for the variations in the selected body size using the Region of interest manager tool. The average of each group was taken and the number of apoptotic cells for each embryo was normalized over the average area of the group.

DNA of each embryo was collected to perform genotyping. Embryos were first euthanized with tricaine after which DNA extraction was performed. Next, PCR was performed on this DNA using the ford protocol (addendum 2), Cmg35_F and Cmg35_R primers and the KAPA2G Robust HotStart ReadyMix Ford master mix (see addendum 3). PCR products could be placed on a

capillary gel electrophoresis that can detect the 13 base pair deletion in case of mutated *brca2* (see addendum 4).

4.2.2.4 Eye size test

For the eye size test the same strain was used as the AO assay (offspring of brca2$^{cmg35/+}$ heterozygotes). At 6hpf, embryos were collected and incubated with 5µM olaparib. The solution with olaparib was renewed at 52hpf. At 72hpf the larvae were sedated using tricaine and placed laterally on methylcellulose droplets. Visualization of the larvae was done with a Leica M165FC stereomicroscope at a 4x magnification. Again, ImageJ was used, this time to measure the area of the eye as a quantitative marker for growth malformations. Genotyping of the *brca2* gene was done as described above.

5. Results

5.1 Optimization xenograft procedure

5.1.1 Cell dissociation

An essential step in the xenograft procedure involves cell dissociation upon labeling. Initially, the protocol as described by Fior *et al.* using EDTA mediated dissociation of cells was conducted. However, we experienced low viability after dissociating cells (figure 13). In addition, injection of these cells proved troublesome, as cells clotted causing clogging up of the needle to be a continuous issue. After adding EDTA, cells were scraped from the surface and collected. Toluidine blue staining showed that scraping these cells was quite harmful, as many cells were dead after collection. During cell death, DNA is set free from cells and DNA is a highly viscous substance. Thus, low viability leads to a more viscous cell substance which causes increased clogging up of the injection needle. Furthermore, the relatively large size of the PANC-1 cells might further accelerate clogging up of the injection needle in these conditions. Lastly, we noticed that EDTA dissociated cells were still clustered in relatively large groups, which can also cause needle clogging. In order to improve cell viability, we used two additional methods to dissociate the cells with as goal optimization of the protocol in order to obtain both more single cells and a higher viability. This would ultimately lead to a decreased clogging up of the needle. The viability obtained through the different methods are displayed in figure 13.

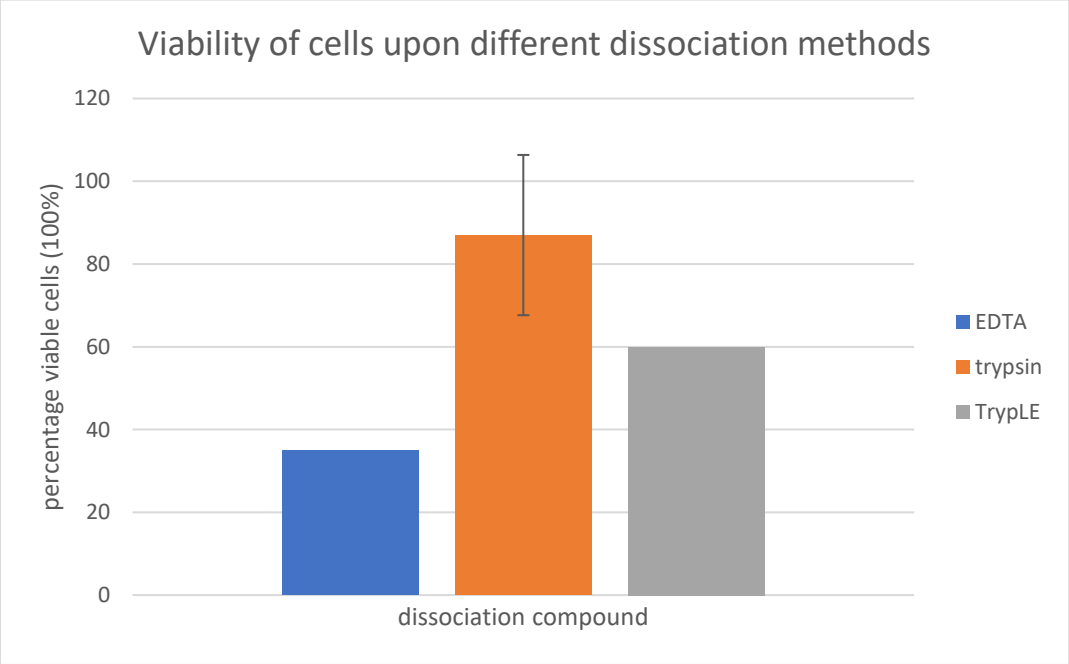

Figure 13: *Viability of cells upon different dissociation methods displayed in percentages. For the EDTA and TrypLE method, one data point was included. For the trypsin method two data points were included. The error bar indicates 95%CI.*

As mechanical dissociation proved too aggressive and ineffective, we next tried enzymatic dissociation protocols. In the second method we used trypsin. Trypsin is an enzyme that cuts peptides between lysine and arginine. Trypsin dissociation is a known technique to split and harvest cells. It was no longer necessary to scrape the cells, causing less debris and dead cells. A downside of using trypsin for too long is that it can become toxic for the cells as it degrades the membranes of these cells. To avoid this toxicity, we added DMEM after dissociation in order to

inhibit the trypsin. Because trypsin impairs the membrane we investigated a third substance to harvest cells. However, the goal was to create a tumor in the zebrafish larvae so once the cells are injected they have to be able to recognize other human cells to form a tumor.

The last method also involves enzymatic digestion. Here, trypsin was replaced with TrypLE. This is another enzyme that is known to be more gentle to cells, is easy to use and room-temperature stable. Like trypsin, the cells did not need to be scraped and the additional step for inhibiting the enzyme function was not necessary.

We wanted to compare these three methods in order to find the most suitable protocol. Unfortunately, the Corona crisis did not allow further experiments leaving us with only three data points for the PANC-1 cell line. Table 1 displays the viability obtained in the three datapoints. The first attempt of conducting the trypsin method the cells were counted manually and some mistakes were made resulting in a low viability (74%) displayed in table 1. The second data point was obtained when conducting the trypsin method a second time. Cells were counted both manually and automatically and results are displayed in table 1. When counting manually, a lower viability was seen (83%) compared to the automatic count (91%). The last data point was obtained through performing the TrypLE method. Cells were only counted manually and viability was very low (62%).

Table 1: *viabilities obtained after dissociation using the trypsin and TrypLE method*

	Data point 1: trypsin	Data point 2: trypsin	Data point 3: TrypLE
Viability (%)	Manually: 74%	Manually: 83% Automatic: 91%	Manually: 62%

After dissociation and collection, cells were quantified. To count the cells, two methods were compared. The first one was counting with a Burker count chamber (manually) and the second one is an automatic count with Luna-II. Using the automatic cell counter would be advantageous as this is much faster than manual counting. After multiple attempts and comparisons between the manual and automatic method, we concluded that the latter was too inaccurate. The Luna-II typically underestimated the density of the cells by a factor of 10. However, in this device you have the ability to change parameters such as cell size and cluster analysis. We therefore planned to perform several experiments with the PANC-1 and Mia-Paca-2 cell line in order to get the automatic counting method more reliable. The experiments were unfortunately not completed due to the Corona crisis. In general, there was little variation in the cell density between the different dissociation methods.

5.1.2 Engraftment

We performed some injections of PANC-1 cells in zebrafish larvae that were harvested using the EDTA and trypsin method. We aimed to inject labeled tumor cells in the PVS of the larvae. This required a lot of skills, and therefore I had to perform multiple injections before being proficient enough to inject cells with high accuracy. Figure 14a displays a H&E staining of a fish with tumor cells injected into the yolk sac. Cells are concentrated in the tumour but do not develop a compact structure as expected in a real tumour. For this reason, injection in the PVS was desired like shown in figure 14b.

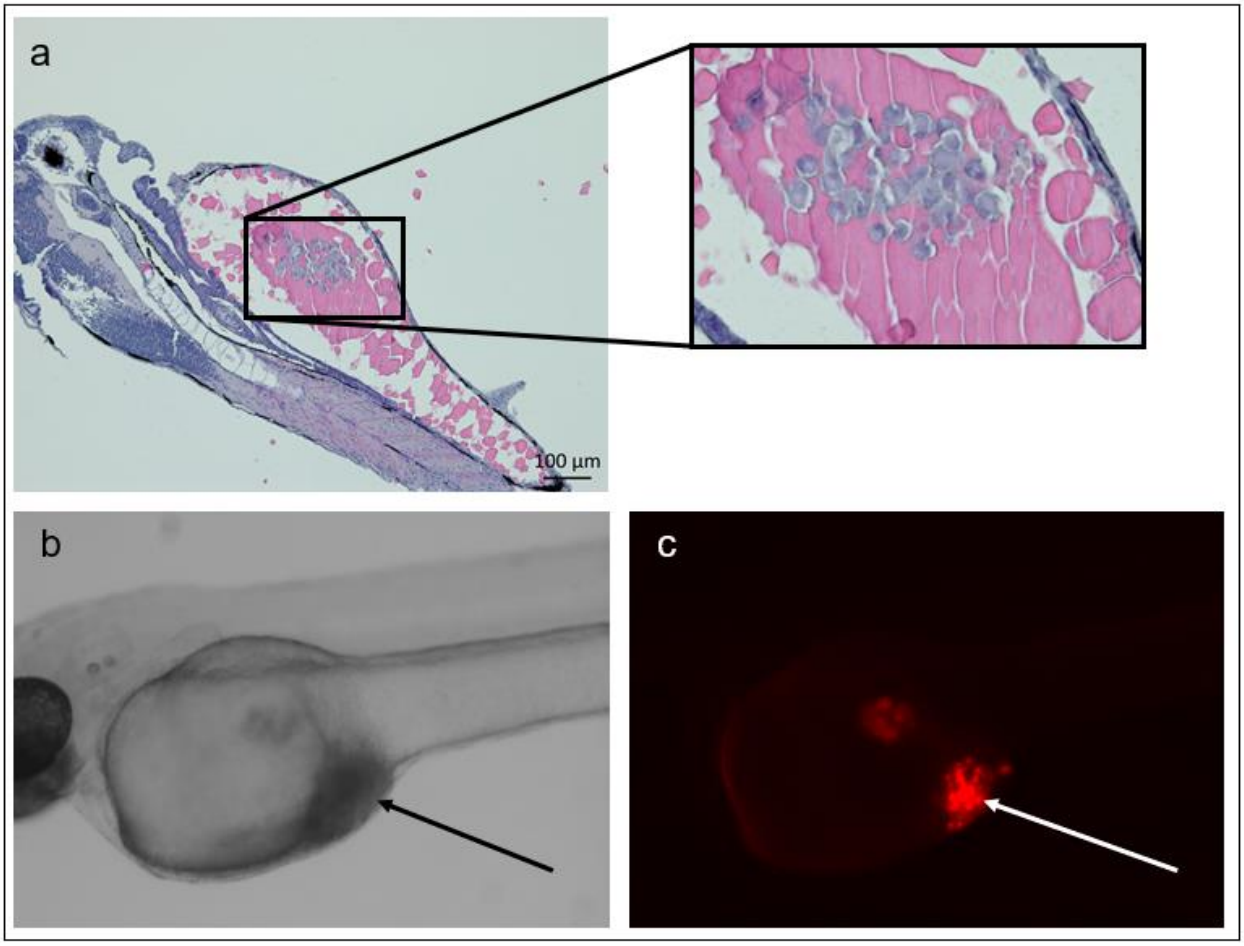

***Figure 14**: zebrafish larvae after PANC-1 injection; **a**: H&E staining of larvae 3dpi injected in yolk sac; **b**: image of larvae 0dpi injected in PVS. Black arrow shows injected cancer cells; **c**: fluorescent image of larvae 0dpi injected in PVS. White arrow shows cancer cells labelled with DiI.*

After several attempts, some injections were successful. In figure 15 you can see a picture of a larvae with PANC-1 cells injected into the PVS 4 days post injection (dpi).

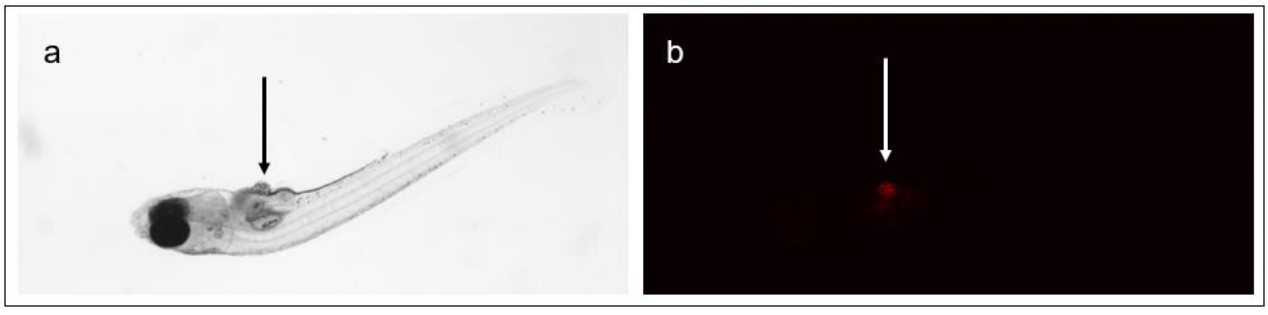

***Figure 15:** 4dpi larvae injected with PANC-1 cells **a**: image of larvae injected in PVS 4dpi. Black arrow shows tumor; **b**: fluorescent image of larvae injected in PVS 4dpi. White arrow shows cancer cells labeled with DiI.*

We were not able to inject Mia-Paca-2 cells as a consequence of time shortage due to the Corona crisis.

5.2 PARPi

PARPi therapy has shown remarkable results in pancreatic cancer patients with *BRCA1/2* mutations[55]. To further accelerate development of novel PARPi compounds, we investigated if zebrafish could be used as an early *in vivo* model to establish PARPi efficacy. To establish this model, several assays were performed like the Rad51 foci assay, acridine orange assay and an eye size test.

5.2.1 DMSO toxicity

In all PARPi experiments DMSO was used as negative control. To check the toxicity of DMSO an experiment was conducted. Larvae were exposed to DMSO in a concentration ranging from 1% to 5% (six larvae per condition). At concentrations of 1% and 2% there were no malformations visible and all larvae were alive with normal phenotype. When 3% DMSO was administered, two larvae were unable to swim straight. This is called a weak phenotype. One larvae had a severe phenotype. This larvae was unable to move even when stimulated, had a curled tail but a heartbeat was present. 4% DMSO caused three dead larvae and all remaining larvae had a severe phenotype and when 5% DMSO was administered to the larvae, only one was still alive but with severe phenotype after incubation. This test suggests that a maximum concentration of 2% DMSO can be administered to larvae to use as negative control. Figure 16 displays the results of the DMSO toxicity test.

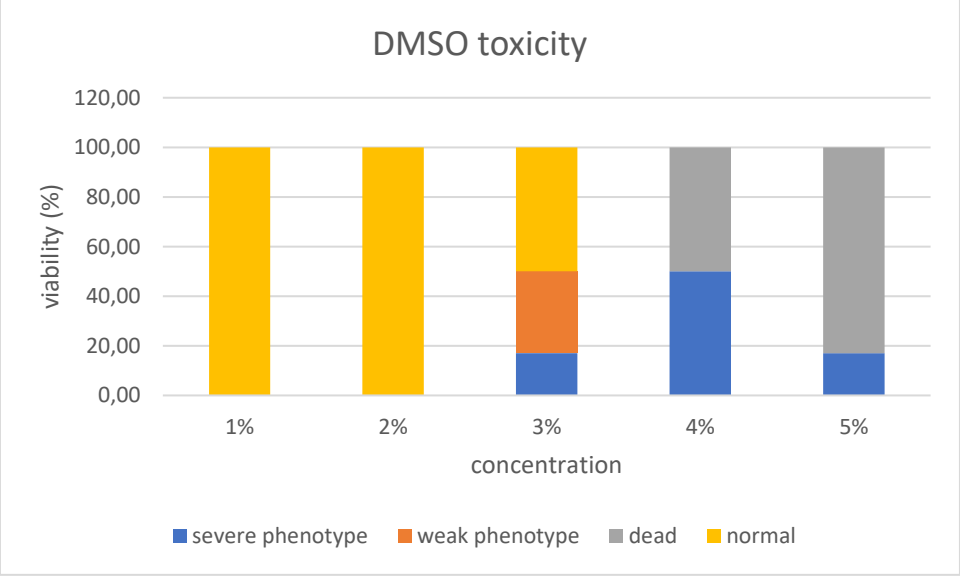

Figure 16: *results of DMSO toxicity test. For each condition 6 larvae were included. Weak phenotype is when larvae are unable to swim straight. Severe phenotype is when malformations occur, larvae are completely unable to swim but heart beat is present.*

5.2.2 Rad51 foci

The Rad51 foci assay measures the amount of HR occurring in cells. To evaluate the efficacy of the tested PARPi, 72hpf larvae (*Tg(EF1a: mCherry-zGem)*^{oki011}) were exposed to 400µM of PARPi for 7h. After 7h all larvae were fixed with PFA. Larvae were cut into sections and an immunohistochemical staining was performed in which anti-Rad51 and anti-mCherry antibodies were used as primary antibodies. Goat-anti-rabbit Dylight 488 antibody and goat-anti-mouse Dylight 594 were secondary antibodies. Figure 17 shows the results of a staining. The Rad51 foci

were counted only in the geminin positive cells (red cells) as these cells are in S-/G2- phase with active HR pathway. This staining was demonstrated in olaparib treated fish at a concentration of 400µM.

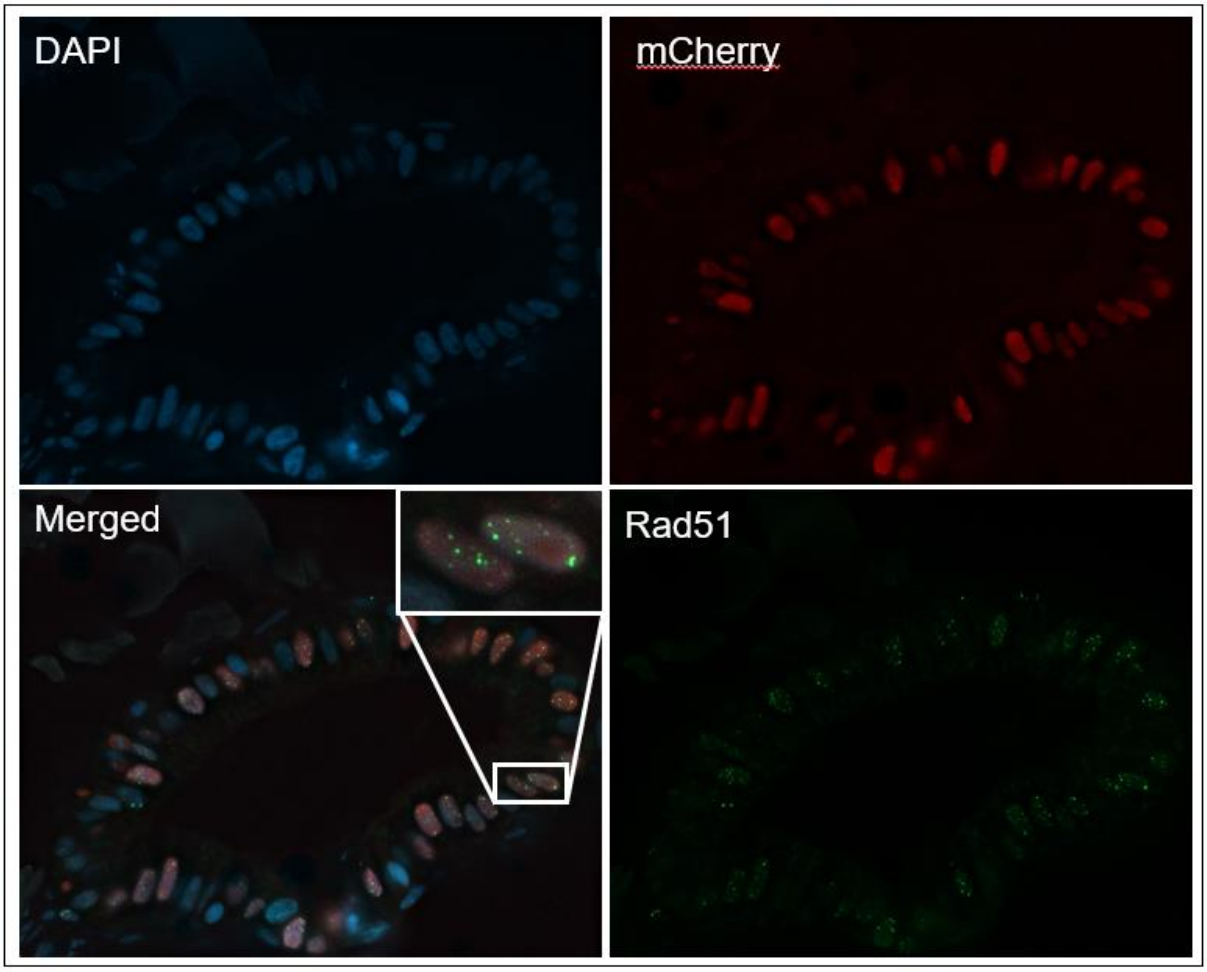

***Figure 17**: immunohistochemical staining. Upper left: DAPI staining of nuclei in blue; upper right: geminin positive cells in red; bottom left: merge of all staining; bottom right: Rad51 foci are bright green dots*

5.2.2.1 PARPi comparison

Besides olaparib, several other PARPi are finding their way in clinical settings. In order to see if the Rad51 foci assay could observe differences in PARPi potency of existing compounds, the Rad51 foci assay was conducted after application of all clinically available PARPi (rucaparib, veliparib, niraparib and talazoparib) to zebrafish embryos. A DMSO condition was included as negative control and generated 1,0±0,8 foci per geminin positive cell. Results were normalized for the amount of geminin positive cells and are stated in figure 18. At a concentration of 400µM olaparib induced eight times more foci per geminin positive cell compared to the DMSO control (8,3±1,8 foci/cell). Talazoparib and niraparib generated a comparable increase in amount of foci per cell (talazoparib: 8,0±2,2 foci/cell and niraparib: 8,0±1,2 foci/cell). Veliparib induced merely three times more foci per cell compared to the DMSO control (2,6±0,8 foci/cell). Surprisingly, rucaparib induced around threefold more foci per cell when compared to DMSO (3,1±1,8 foci/cell) which was lower than expected.

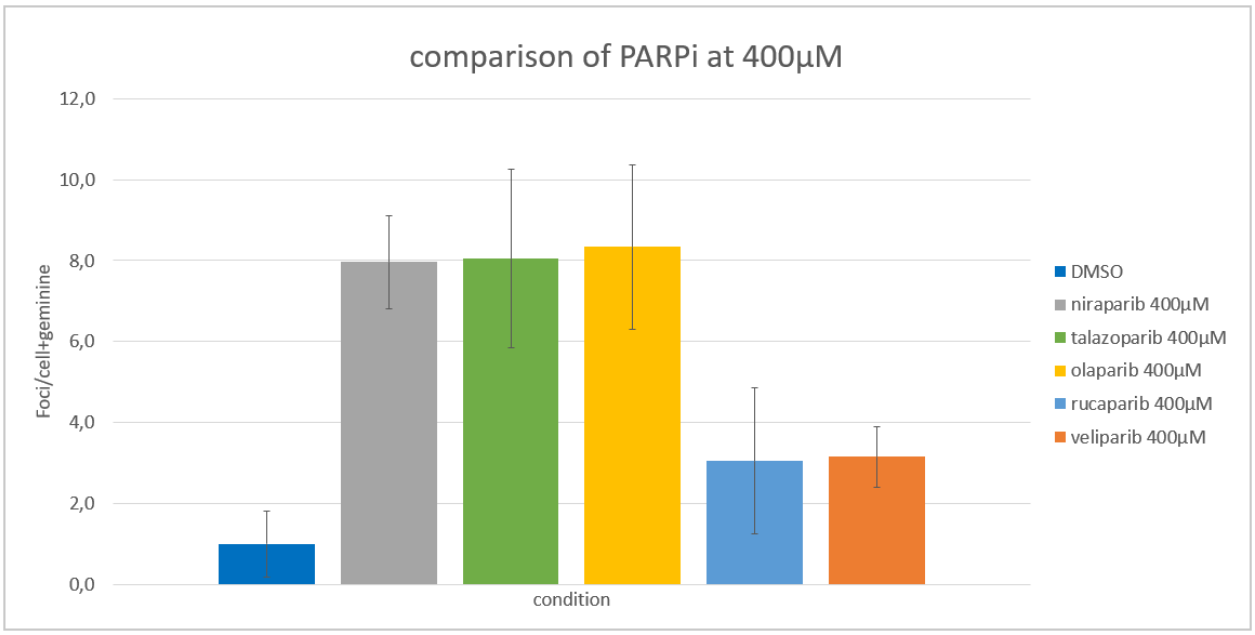

Figure 18: *Comparison of all clinically available PARPi. Error bars display 95% CI. At least 3 larvae were included per condition.*

5.2.2.2 Assessing potency of talazoparib

Rucaparib and veliparib leveled out at approximately three times more foci/cell. Likewise, olaparib, talazoparib and niraparib approximately displayed the same increase in Rad51 foci compared to DMSO at a concentration of 400µM. A plateau seemed to occur but talazoparib is known to be a more potent PARPi than olaparib. Therefore, the Rad51 foci assay was performed for olaparib and talazoparib at much lower concentration (5µM) to confirm the higher potency of talazoparib. Figure 19 shows the results of the experiment for olaparib and talazoparib at a concentration of 5µM.

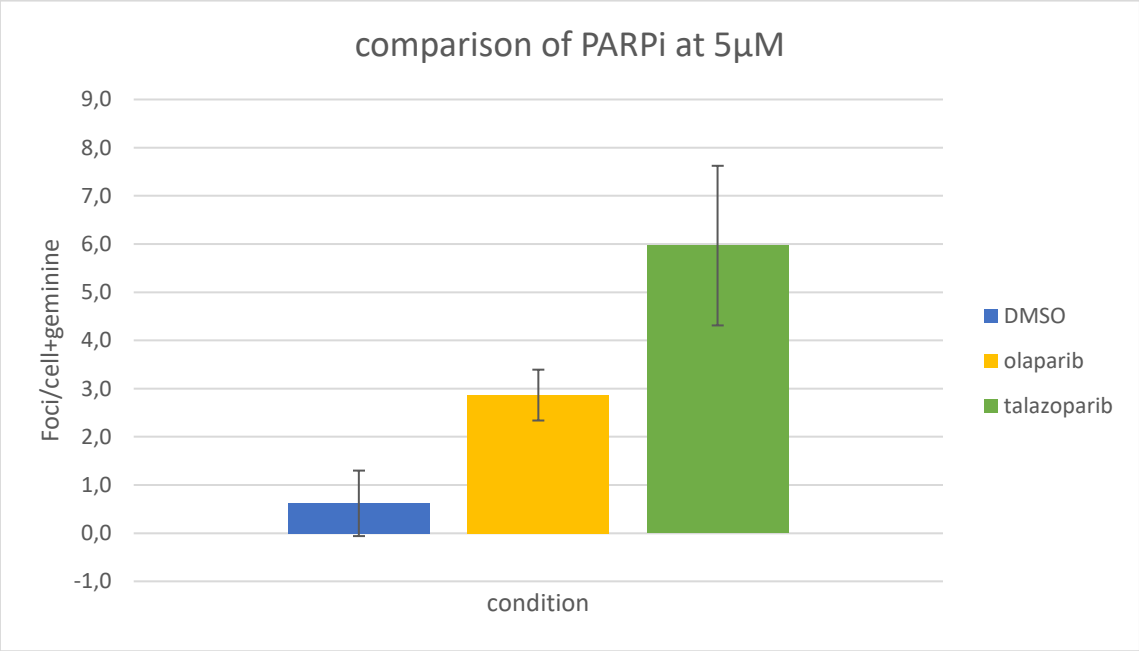

Figure 19: *Rad51 foci count of olaparib and talazoparib at 5µM concentration. For each condition 4 larvae were included. Error bars display 95% CI*

It indicates that olaparib is indeed less potent at a lower concentration than talazoparib. Olaparib induces almost three times more Rad51 foci per cell (2,9±1,5 foci/cell) than DMSO but talazoparib generates a six fold of Rad51 foci (6,0±1,7 foci/cell) at this lower concentration.

5.2.2.3 Dose response

In order to further understand the potency of each PARPi, we aimed to perform a dose response of all five PARPi. Unfortunately, due to the Corona crisis, the experiments were not completed. Larvae were already incubated with rucaparib and veliparib. Sections were made and a staining was performed. Due to a mistake in the staining of the rucaparib slides, the staining failed and needed to be repeated. Some veliparib conditions were successfully stained and thus could be analyzed. In figure 20 the dose response results of Veliparib are displayed.

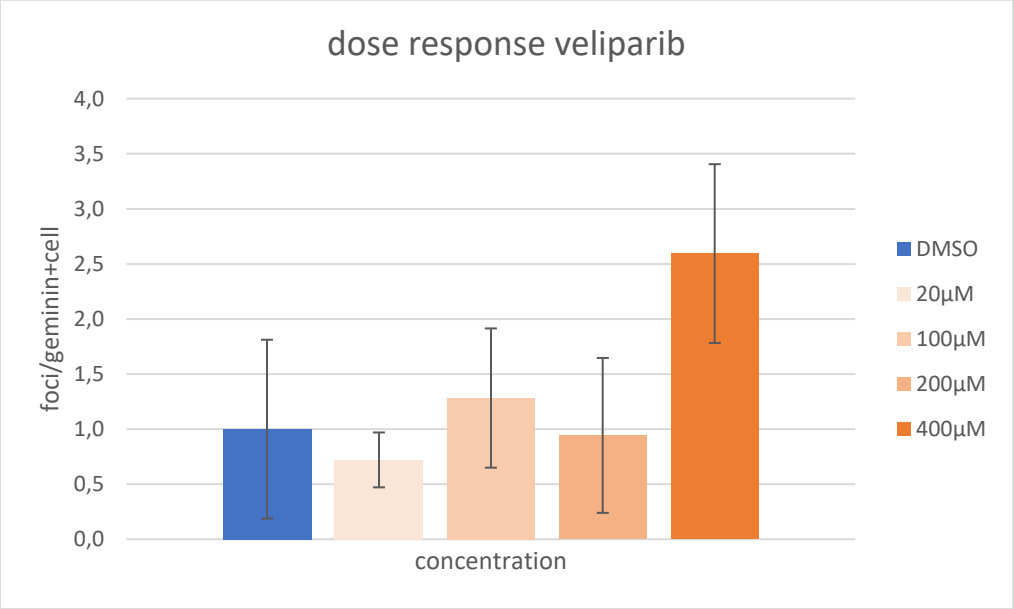

Figure 20: *dose response veliparib. For all conditions 4 larvae were included. Error bars display a 95% CI.*

As veliparib already shows a low signal at a concentration of 400µM (figure 18), signals at even lower concentrations (20-200µM) seem not distinguishable from background signal (noise + background HR repair). Error bars are quite sizeable at all concentrations. The Rad51 foci assay has some variability, which makes it harder to observe statistical significant changes, especially in the lower concentration range. To observe statistically significant data for veliparib more data points should be included. In addition, we aimed to test a concentration of 800µM, but this has not yet been performed.

5.2.3 Acridine orange assay

In addition to the Rad51 foci assay, we were interested in how PARPi interact with zebrafish that are deficient in HR. Therefore, we performed the acridine orange staining. The goal was to check if there is a difference in apoptosis after PARPi administration between wild type and mutant *brca2* fish. The 6hpf larvae (offspring of *brca2*$^{cmg35/+}$ heterozygotes) were incubated for 24 hours with 5µM of olaparib. This is enough time for olaparib to cause cell death in *brca2* mutated cells due to accumulation of DNA damage. Figure 21 shows an acridine orange staining of a wild type and a mutant fish.

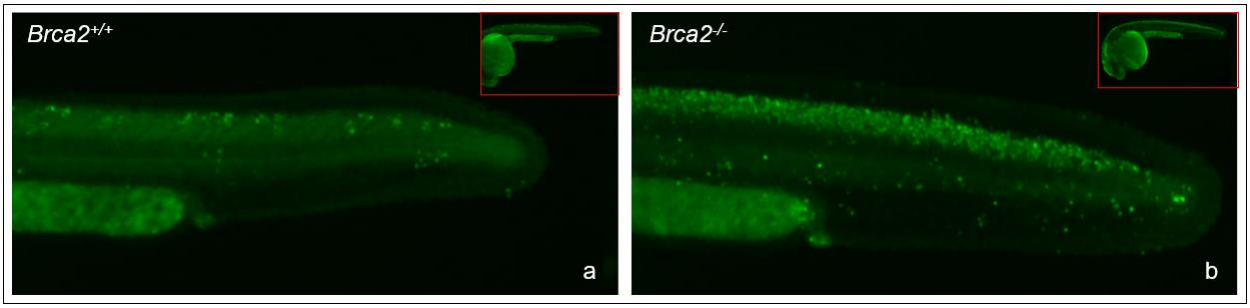

***Figure 21**: AO staining. Bright green dots are apoptotic cells; **a**: AO staining of a wild type larvae; **b**: AO staining of Brca2$^{-/-}$ mutant*

Figure 22 shows the fold change of apoptotic cell counts of *brca2*$^{-/-}$ mutant larvae treated with olaparib and *brca2*$^{+/-}$ heterozygote larvae treated with olaparib normalized against olaparib-treated wild type larvae. Heterozygotes had an increased number of 1,3±0,5 apoptotic cells compared to wild type but it was not statistically significant (p-value:0.3). *Brca2*$^{-/-}$ mutant larvae had a 1,9±0,4 increase of apoptotic cells with a p-value of 0,005 which is statistically significant. Thus olaparib only induces the amount of apoptotic cells in mutant larvae and not in heterozygotes.

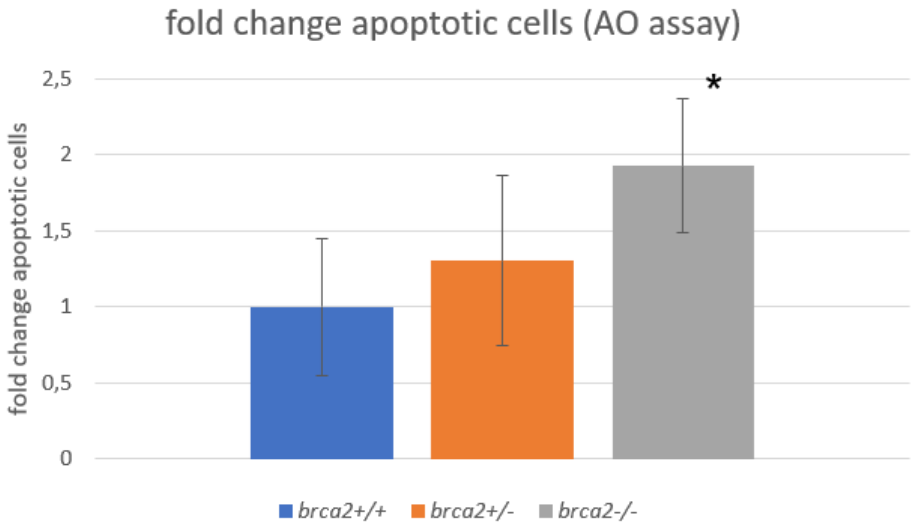

***Figure 22:** result of acridine orange staining normalized against wild type larvae. Error bars display the 95% CI. 4 wild type larvae, 5 heterozygote larvae and 5 mutant larvae were included. (*p<0,05)*

The next graph (figure 23) shows the fold change of apoptotic cells of olaparib treated *brca2* mutants, heterozygotes and wild types, normalized against their untreated counterpart (0µM olaparib). Wild type larvae displayed a 2,3±0,1 increase of apoptotic cells, with a p-value of 0,054. Treated heterozygotes have a 3,0±1,3 increase compared to control heterozygotes with a p-value of 0,002. The mutant larvae that were treated have an increased apoptotic cell count of 3,1±0,7 compared to the control mutants with a p-value of 0,006. Thus the increase of apoptosis in the wild type larvae is not significant however the increases of apoptotic cells in the heterozygote and mutant larvae are statistically significant.

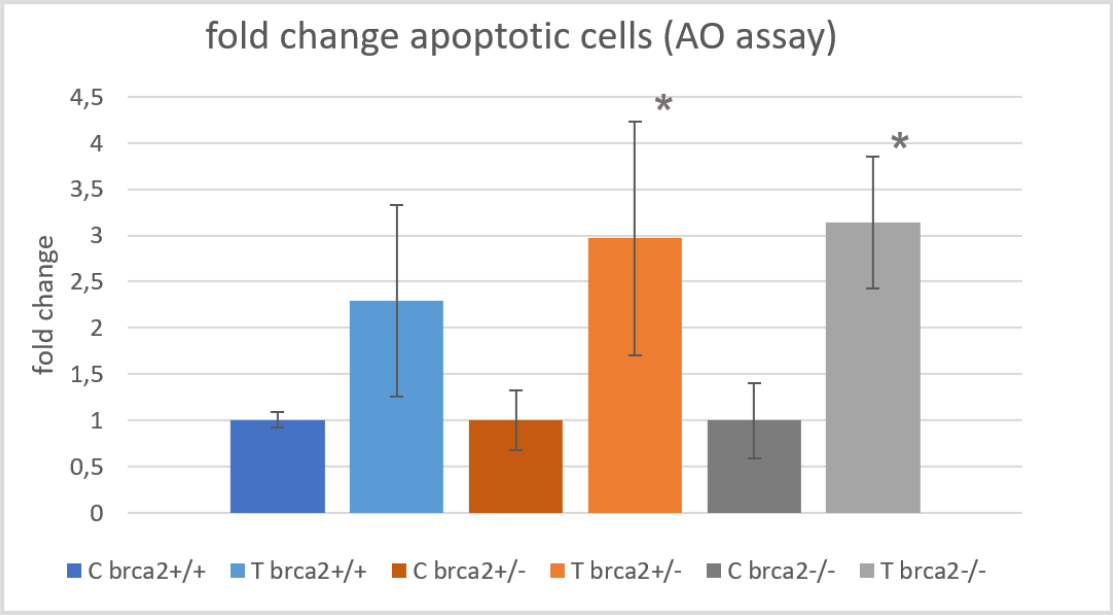

Figure 23: *AO assay of WT, heterozygote and mutant larvae. Fold change of apoptotic cells for treated larvae normalized against untreated counterpart. Error bars display 95% CI. At least 3 WT larvae were included, 5 heterozygotes and 2 mutants. C in legend stands for control; T stands for treated. (*p<0,05)*

5.2.4 Eye size test

Lastly, we were interested in the long term effects of PARPi exposure. Therefore, we developed a malformation experiment. Larvae (offspring of *brca2*$^{cmg35/+}$ heterozygotes) were incubated with 5µM olaparib for 72 hours after which we expected to observe malformations. In *brca2*$^{+/+}$ wild type and heterozygous larvae we detected no malformation. Nonetheless, malformations like curved tail, smaller eyes and skeletal deformation of the skull were observed in mutant larvae. To objectively quantify the malformations, the size of the eye was measured. Figure 24 shows a *brca2*$^{+/+}$ wild type and a *brca2*$^{-/-}$ mutant larvae both after 72h of incubation with 5µM olaparib. The smaller size of the eye is already visible alongside malformations in the head and a curled tail.

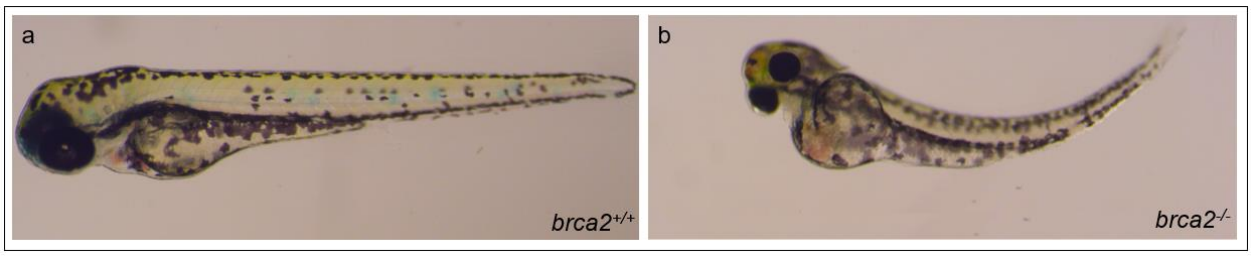

Figure 24: *zebrafish larvae after malformation test;* ***a****: wild type larvae after 24h incubation with 5µM olaparib;* ***b****: brca2 mutant larvae after 24h incubation with 5µM olaparib*

Figure 25 shows the results of the eye size experiment. The results were normalized against wild types. Heterozygous fish have only slight reduction in the size of the eye (0,9±0,1 fold change) but with no statistical significance (p-value is 0,4). The size of the eye of the mutant fish are halved (0,5±0,1 fold change) and statistical significance is proven (p-value: 0,0005).

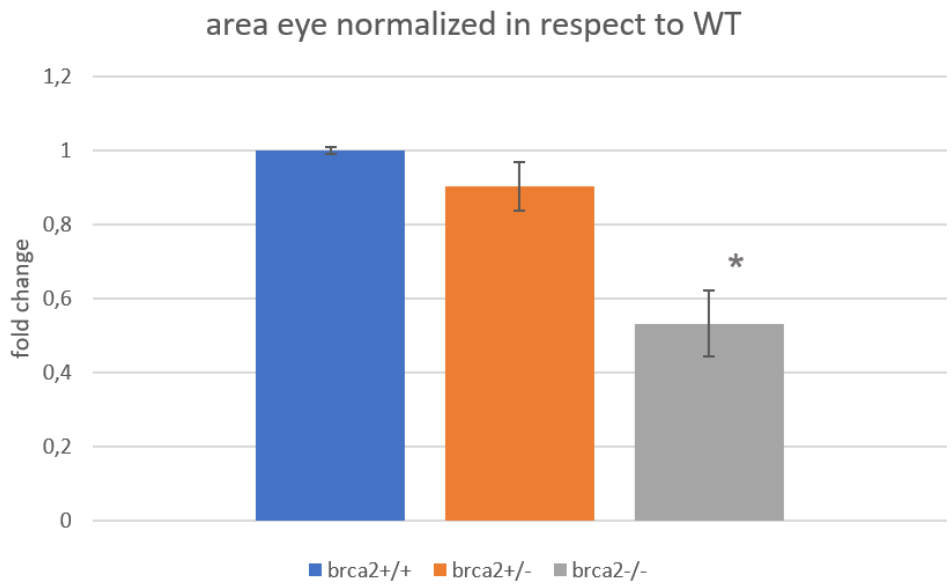

Figure 25: *eye size normalized against wild types. Error bars display the 95% CI. 2 WT larvae were included, 12 heterozygotes and 9 mutants. (*p<0,05)*

6. Discussion

6.1 Zebrafish embryonic xenografts

6.1.1 Cell dissociation

Pancreatic cancer is the 11th most common cancer and the 7th highest cause of cancer related deaths worldwide[8]. Pancreatic cancer has a poor prognosis with the five-year survival rate around eight percent and most patients dying within six months after diagnosis. This is mainly due to late diagnosis, rapid progression with early metastasis, refractoriness to therapy and lack of therapeutic approaches. Treatment exist of surgery and chemotherapy. However, due to late diagnosis, many patients have already developed distant metastases. Treatment is these palliative patients consist purely of symptom control. Nowadays, the choice of therapy is based on the condition of the patient. To improve prognosis, more personalized therapy approaches are crucial. Up to date, the response to therapy is unpredictable. Patient derived xenografts (PDX) in mice are now used to predict response to therapy in patients[85]. Yet mice are linked with high costs and long engraftment time, time a pancreatic cancer patient does not have. Using zebrafish, these problems can be solved.

To build a zebrafish PDX platform, we based ourselves on the protocol of Fior *et al.* Besides their high-quality research[80], they also distinguish themselves from many articles by injecting into the PVS instead of the yolk sac. They argue that injection in the yolk sac is not suitable for xenograft experiments as cells will not perform clusters and articles using this method have never performed H&E staining to monitor cell viability of such xenografts (personal communication).

For our optimization, we used the commonly known PANC-1 human pancreatic cancer cell line. During the labeling process of these PANC-1 cells we observed several difficulties. For one, dissociation of PANC-1 cells with EDTA, like described by Fior *et al.*[80], resulted in numerous dead cells. Moreover, attempts to inject these cells resulted in needle clogging. There are several possible reasons as to why this is.

EDTA is a Ca^{2+} chelator that removes the calcium that intregrins need to maintain cell adhesion and is well-known to be a gentle method for dissociating cells. Fong *et al.* proved that by using EDTA the cell surface integrity[86] is intact but detachment of adherent cell occurred in barely 50% of all cells. To detach all cells from the surface of the flask a cell scraper was used. Scraping of cells was damaging causing lower viability. In addition, DNA is a viscous substance that is released during apoptosis causing higher viscosity when lower viability is obtained. Another explanation is that pancreatic cancer cells may be more adherent than other cell lines causing the needle to clog up more frequently. For better engraftment with less clogging up of the needle new methods were investigated.

Vlecken *et al.*[87] was able to perform successful engraftment of PANC-1 cells after using trypsin to dissociate cells. Trypsin is an often used enzyme in cell culture maintenance. However, trypsin is more aggressive and is toxic when administered for too long a period of time. In addition, trypsin causes degradation of cell surface proteins which results in lower cell recovery after trypsinization[88]. This might prove detrimental for the capacity of injected cells to form tumor clumps in the xenograft. To avoid toxicity of trypsin, DMEM was added after cell dissociation. DMEM is enriched with fetal bovine serum (FBS) which contains protease inhibitors, like 1α-antitrypsin, that

inhibit trypsin. The cell scraping was no longer necessary due to the higher yield of cells resulting in less debris and thus higher viability after cell dissociation.

The trypsin method resulted in increased viabilities. The first time doing this experiment, some mistakes were made. A too low confluence of cells was used to start and there was inadequate resuspension. These mistakes are a consequence of lack of experience. When repeating this protocol those mistakes were avoided resulting in more cells per mL with higher viability.

To obtain even higher viabilities and avoid cleaving of cell surface proteins, a third method was tested. In this method, TrypLE was used. This is a mixture of enzymes, less aggressive than trypsin, thus thought to induce higher viability. It is known that TrypLE is the most advantageous cell dissociation reagent[88] as it does not affect cell surface antigen expression. Tsuji *et al.* demonstrated that, compared to trypsin, cell recovery with TrypLE is higher[88]. PANC-1 cell dissociation using TrypLE was only conducted once due to lack of time caused by the Corona crisis. This resulted in a high number of cells per mL but with lower viability (61%) contradicting the findings of Tsuji *et al*. It is uncertain why the viability was that low. More data points have to be manufactured to make a conclusion. A possible explanation is that the used TrypLE batch was outdated and purchase of a new batch was required.

Our ambition was to provide more data points and investigate all protocols in order to select the best protocol for harvesting and labeling cells. However these three data points were the only ones obtained. Additionally, the goal was to compare the three methods between PANC-1 and Mia-Paca-2 cells. Unfortunately, this was not possible due to lack of time as a consequence of the Corona crisis.

To further optimize the protocol, manual counting of cells can be replaced by an automatic count with Luna-II. Automatic counting is advantageous as it is less time-consuming. However, after several attempts, it was concluded that the automatic count was too inaccurate compared to manually counting the cells. The Luna-II underestimated the density of cells by a factor of ten. As several parameters in the Luna-II device can be adjusted, it was our goal to optimize the counting protocol of the device. Experiments were set up but were not completed due to time restraints caused by the Corona crisis. Several parameters of the device, like cell size and cluster analysis, can be adjusted. A concentration would be counted manually. The cell size parameter in Luna-II would be enlarged to correctly count all PANC-1 cells and cluster analysis would be widened to include all cells even when clustered together. Adaptations in these parameters would be continued until the cell count and viability resembles the reality. Once optimized, a relevant concentration curve consisting of at least five data points would be tested. Each concentration point would have to resemble a true cell count with correct viability (would be checked with manual counting). If not, parameters would require readjustment until cell count and viability resemble true values. This protocol would be done for both the PANC-1 and the Mia-Paca-2 cell line.

6.1.2 Engraftment

The most challenging part of the engraftment protocol is the injection as it requires countless hours of practice. A time period of one week is required for each injection exercise due to the complex protocol in which cell culture and zebrafish breeding need to be aligned. 48hpf larvae are approximately 3mm long so injection has to be done using a microscope. Injection in the yolk sac

is quite easy as it is a large structure but the tumor loses its compactness when injected into the yolk sac (see figure 14a). The PVS is a small structure in the larvae so precise injection is of great importance to ensure the tumor remains its characteristics like compactness of cells[80,87,89,90]. Learning to xenograft is preferably done with cells that easily engraft such as the HCT116 cells. Engraftment of PANC-1 cells is arduous as PANC-1 cells are bigger in size thus increase the chance of clogging up the needle. After many hours of practice, successful engraftments of PANC-1 cells were made (figure 14). However, after several days many larvae developed edema. Edema were most likely caused by an obstructed PANC-1 cell in the blood vessel consecutive to an escaped cell. As Mia-Paca-2 cells are smaller in size (see figure 26), we hypothesized that these cells would cause less formation of edema after engraftment.

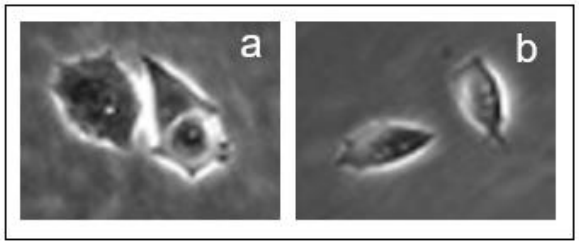

Figure 26: *PANC-1 and Mia-Paca-2 cell lines obtained from ATCC website;* ***a:*** *PANC-1 cells;* ***b:*** *Mia-Paca-2 cells*

Once we have optimized the engraftment protocol for both PANC-1 and Mia-Paca-2 cells, tumor response to compounds can be compared between the two cell lines. The Mia-Paca-2 cell line is known to be more sensitive to gemcitabine and our goal was to confirm this with xenografts. However, only a handful successful engraftments were made with PANC-1 cells. The Mia-Paca-2 cell line was cultured although no engraftments could be performed using this cell line because of the Corona crisis.

6.2 PARPi

With constant development of novel PARPi compounds it is crucial to have a cheap, accurate and fast *in vivo* model to investigate PARPi efficacy. Hence, to further accelerate development of PARPi compounds, we investigated if zebrafish could be used as an early *in vivo* model to establish PARPi efficacy. As 10% of pancreatic cancer patients are known to have mutations in HR genes[54], PARPi therapy might prove beneficial to these patients. PARPi therapy has shown remarkable results in pancreatic cancer patients with *BRCA1/2* mutations[55]. Additionally, non-pancreatic cancer patients with defects in *BRCA1/2* can benefit from PARPi therapy.

When larvae are exposed to olaparib, DNA DSBs develop and are subsequently repaired by the HR pathway. The efficacy of olaparib to induce HR can be quantified by counting Rad51 foci. Larvae of the *Tg(EF1a: mCherry-zGem)*^{oki011} strain have fluorescently labeled geminin making it possible to determine cell cycle phase. Geminin is a DNA replication inhibitor that is only present during the S- and G2- phase of the cell cycle. HR is only performed in this phase of the cell cycle. So when DSB are formed, Rad51 foci are assembled. Larvae were incubated with olaparib for 7 hours, fixated and section were made which were subsequently stained with a immunohistochemical staining against geminin and Rad51.

All five clinically available PARPi (olaparib, niraparib, rucaparib, veliparib and talazoparib) are tested for their capacity to induce Rad51 foci at a concentration of 400µM. All five PARPi induced

Rad51 foci at this concentration but in variable amounts. Olaparib, talazoparib and niraparib appeared to have similar high Rad51 foci counts at this concentration. Rucaparib and veliparib showed low increases of Rad51 foci suggesting lower efficacy opposed to olaparib, talazoparib and veliparib. The manner of inhibiting PARP can differ between PARPi. Some PARPi mainly work by inhibiting the catalytic cavity of the protein and others particularly by trapping the PARP protein onto damaged DNA[64]. The trapping PARPi are thought to induce more toxicity and thus be more efficient. Murai *et al.* previously showed that indeed olaparib, talazoparib and niraparib have higher trapping potencies than veliparib[91]. The most potent trapping compounds are the strongest anticancer compounds and, as mentioned previously, veliparib has only moderate effects in anticancer therapy[67]. Veliparib is known to mainly inhibit the catalytic cavity of PARP[64]. This assay showed that indeed veliparib induces less Rad51 foci which is probably caused by less potent trapping. In contrast to predictions[92], rucaparib seems to be less potent for inducing Rad51 foci. Consistent with this, the FDA prescribed the recommended dose for rucaparib at twice the dose of olaparib. This suggests that *in vivo* models might be more suitable to display PARPi toxicity than cell models.

Talazoparib is thought to be more potent than olaparib. Because of the equal increase of Rad51 foci in olaparib and talazoparib at a high concentration (400µM), we suspected that a maximum Rad51 foci signal was obtained. Therefore this assay was repeated at a lower concentration (5µM). This experiment confirmed that talazoparib had indeed a higher efficacy (6,0±1,7 foci/cell) than olaparib (2,9±1,5 foci/cell).

A dose response was set up to investigate the highest potency of each individual PARPi. Unfortunately, only the dose response of veliparib could be investigated due to time restraints. In this dose response, concentrations ranged between 20µM and 400µM. With the exception of 400µM, all other concentrations were unable to show a statistically significant difference with untreated DMSO controls. A possible explanation for this could be that the sensitivity of the Rad51 foci assay is inadequate at lower concentrations of this PARPi, resulting in higher error bars. This experiment would have been repeated to increase number of data points and reducing the error bars.

In addition to the Rad51 foci assay, we were interested in how PARPi interact with zebrafish that are deficient in HR. Therefore, we performed the acridine orange (AO) assay as it has already been proven that AO assays can be used to investigate toxicity of a compound in *brca2*$^{-/-}$ mutant fish[93]. The goal was to check if there is a difference in cell death after PARPi administration between *brca2*$^{+/+}$ wild type and mutant fish. Chronic exposure indeed caused increased cell death in mutant *brca2*$^{-/-}$ larvae compared to wild type larvae. This confirms the synthetic lethality caused by the PARPi in cells with deficiencies in.

Lastly, we were interested in the long term effects of PARPi exposure and we performed a malformation test. Offspring of *brca2*$^{cmg35/+}$ heterozygotes are chronically (72h) exposed to 5µM olaparib. No malformations were observed in *brca2*$^{+/+}$ wild type and *brca2*$^{+/-}$ heterozygous larvae. However, chronic exposure in *brca2*$^{-/-}$ mutant larvae is cytotoxic due to induced genomic instability and causes malformations like curled tails, skeletal deformations of the skull and a reduced eye size. The reduction in size of the eye is statistically proven in *brca2*$^{-/-}$ larvae compared to wild type larvae. This proves the synthetic lethality of the PARPi in *brca2*$^{-/-}$ mutant larvae.

The strain used in this experiment (offspring of *brca2*$^{cmg35/+}$ heterozygotes) is only mutated in the *brca2 gene.* Many other cancer cell lines and tumors have mutations in secondary genes but in this zebrafish strain no mutations in secondary genes are present. During pre-clinical development of PARPi, these secondary mutations might occlude results expected from PARPi. Having a model organism with a single gene defect allows for observation of the intended effect caused by the PARPi, without companionship of confounding factors generated by mutations in secondary genes.

7. General conclusion

The aim of this master thesis was twofold. The first goal was to establish a zebrafish embryonic model to investigate anticancer treatment for pancreatic cancer. The second goal was to establish an *in vivo* model to investigate PARP inhibitor efficacy. For the investigation of the pancreatic cancer treatment, we aimed to make xenografts of human pancreatic cell lines in zebrafish embryos. Fior *et al.* composed a protocol to engraft human colorectal cancer cells in zebrafish embryos. We investigated engraftment of two human pancreatic cancer cell lines, PANC-1 and Mia-Paca-2. PANC-1 is a commonly known human pancreatic cancer cell line and Mia-Paca-2 is a pancreatic cancer cell line known to be more sensitive to gemcitabine. When conducting the protocol to engraft PANC-1 cells, several difficulties were observed.

Dissociation of the PANC-1 cells using EDTA resulted in low viability levels. Therefore, we used trypsin and TrypLE in additional methods to investigate the most suitable dissociation compound. Highest viabilities were observed when using trypsin as dissociation compound. However, experiments were not ended, leaving us with insufficient data points for both methods. I hypothesize, based on the obtained results and literature studies, that TrypLE would be the most suitable dissociation compound to use.

During engraftment of PANC-1 cells, cells clotted and clogged up the injection needle complicating injection of human pancreatic cancer cells. When the dissociation protocol is optimized, PANC-1 cells would clot less resulting in easier injection. PANC-1 cells are bigger than Mia-Paca-2 cells thus I hypothesize that clogging up of the needle would be less of a problem in the Mia-Paca-2 cells.

I hypothesize that pancreatic cancer cell lines can be engrafted in zebrafish embryos after which anticancer treatment can be tested on these xenografts. However, no reliable conclusions can be made based on the obtained results.

In search of a zebrafish embryonic model to investigate PARPi efficacy, it has been proven that zebrafish are sensitive to PARPi treatment. The HR pathway is upregulated in presence of PARPi which can be visualized with the Rad51 foci assay. All five clinically available PARPi (olaparib, niraparib, talazoparib, veliparib and rucaparib) were tested for their efficacy to induce Rad51 foci. Talazoparib showed highest potency followed by olaparib and niraparib. Veliparib induced fewer Rad51 foci indicating the lower potency of the PARPi. Rucaparib surprisingly showed lower potency to induce Rad51 foci.

When HR is disabled, zebrafish display cytotoxicity to PARPi. This was proven with an acridine orange assay and a malformation test. Zebrafish larvae mutant in the *brca2* gene displayed more apoptotic cells when incubated with 5µM olaparib for 24 hours and displayed malformations when incubated with 5µM olaparib for 72 hours.

To conclude, zebrafish larvae can serve as *in vivo* model for establishing novel PARPi.

8. Poster

FACULTY OF MEDICINE AND HEALTH SCIENCES · UZ GENT · CRIG · CENTER FOR MEDICAL GENETICS GHENT

New perspectives to anticancer therapies using zebrafish embryonic models

Vierstraete Jeroen[1-3,5], Dobbelaere Lore[1,2,5] , Fieuws Charlotte[1-3], Willaert Andy[1,2,4], Vral Anne[3,4], Claes Kathleen[1,2,4]

1. Center for Medical Genetics, Ghent University Hospital, Ghent, Belgium 2. Department of Biomolecular Medicine, Ghent University 3. Department of Human Structure and Repair 4. Zebrafish Facility Ghent 5. Cancer Research Institute Ghent (CRIG)

Zebrafish xenograft model to find best therapy for pancreatic cancer patients

Pancreatic cancer is a devastating disease with a 5-year survival of less than 9%. Current therapies are based on a one-size-fits all regimens but are ineffective in a large part of the population. We propose the use of zebrafish pancreatic xenografts to test for each patient which therapy will be the most effective.

5y survival rate | Early distant metastasis | Resistance to therapy

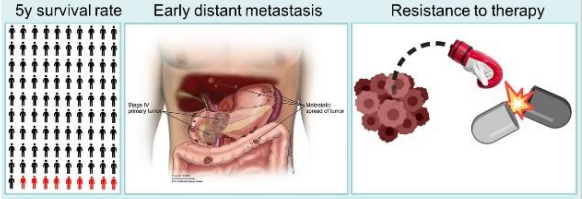

Goal: optimization of xenograft using pancreatic cancer cell lines

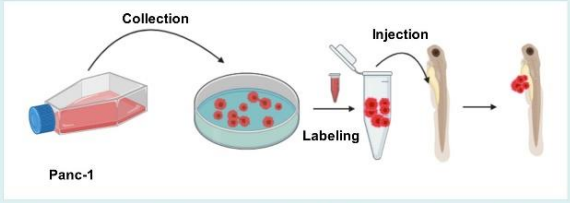

We are currently optimizing xenografting the Panc-1 pancreatic cancer cell line:

- Improving injection skills
- Improving viability during cell collection:

EDTA + scraping	Trypsin	TripLE
+ Less aggressive	- More aggressive	+ Less aggressive
- Poor viability (20-50%)	+ Good viability (+80%)	+ Good viability (+80%)

Result: Panc-1 cells can engraft in zebrafish

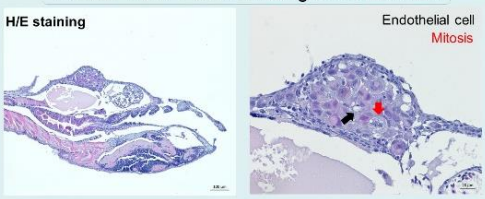

Conclusion

TripLE seems the best technique to dissociate Panc-1 cells for collection. We were able to engraft human Panc-1 cells into zebrafish. The tumor cells appear proliferative and induce angiogenesis. The next step in the optimization process is to graft the Mia-Paca-2 cell line and test the sensitivity of both cell lines to gemcitabine.

Future: testing primary pancreatic tumors to anticancer therapy

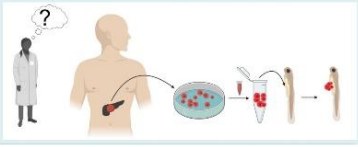

Using zebrafish to assess PARP inhibitor efficacy

PARP inhibitors (PARPi) are compounds that target tumors with mutations in *BRCA1/2* and thus are deficient for Homologous Recombination (HR). They work by converting single strand breaks to double strand breaks that can only be repaired through HR. Failure to do so leads to cell death. New compounds are continuously in development. We wanted to investigate if zebrafish could be used to model PARPi *in vivo*.

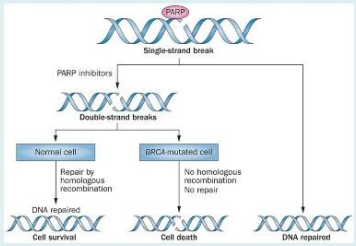

1. Zebrafish exposed for 7h to PARPi display HR repair

72hpf zebrafish embryos are treated with 5 clinically available PARPi and we compared their efficacy. We do this by means of Rad51 foci, which is a marker for HR. All PARPi induce Rad51 foci by trapping PARP and/or inhibiting the catalytic activity of PARP. The curve below shows the foci counts that are normalized to a DMSO condition (negative control).

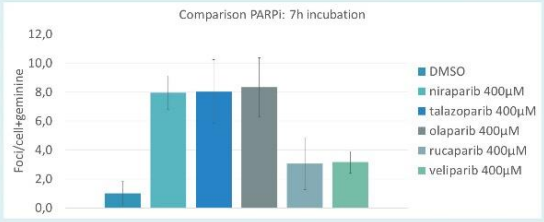

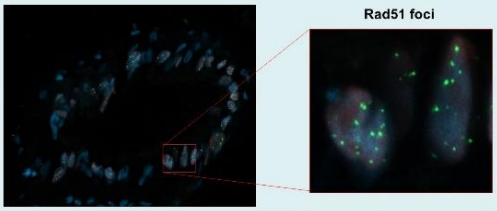

2. *brca2*$^{-/-}$ zebrafish are sensitive to PARPi treatment

Incubation of zebrafish larvae for 72h with olaparib resulted in malformations in the head and tail and reduced surface of the eye in *brca2-/-* larvae. These malformations are not seen in *brca+/+* larvae.

Conclusion

Our findings are that zebrafish embryos can be used to assess PARPi efficacy. Olaparib, talazoparib and niraparib are the most effective PARPi. Olaparib incubation for 72 hours resulted in malformations in the eye, head and tail of the larvae.

9. Reference list

1 Henry, B. M. *et al.* Development of the human pancreas and its vasculature - An integrated review covering anatomical, embryological, histological, and molecular aspects. *Ann Anat* **221**, 115-124, doi:10.1016/j.aanat.2018.09.008 (2019).

2 Laugier, R., Bernard, J. P., Berthezene, P. & Dupuy, P. Changes in pancreatic exocrine secretion with age: pancreatic exocrine secretion does decrease in the elderly. *Digestion* **50**, 202-211, doi:10.1159/000200762 (1991).

3 K., V. in *gezondheidsplein* (2020).

4 Cheng, J. Y., Raghunath, M., Whitelock, J. & Poole-Warren, L. Matrix components and scaffolds for sustained islet function. *Tissue Eng Part B Rev* **17**, 235-247, doi:10.1089/ten.TEB.2011.0004 (2011).

5 Jansson, L. *et al.* Pancreatic islet blood flow and its measurement. *Ups J Med Sci* **121**, 81-95, doi:10.3109/03009734.2016.1164769 (2016).

6 Brereton, M. F., Vergari, E., Zhang, Q. & Clark, A. Alpha-, Delta- and PP-cells: Are They the Architectural Cornerstones of Islet Structure and Co-ordination? *J Histochem Cytochem* **63**, 575-591, doi:10.1369/0022155415583535 (2015).

7 Ballian, N. & Brunicardi, F. C. Islet vasculature as a regulator of endocrine pancreas function. *World J Surg* **31**, 705-714, doi:10.1007/s00268-006-0719-8 (2007).

8 Rawla, P., Sunkara, T. & Gaduputi, V. Epidemiology of Pancreatic Cancer: Global Trends, Etiology and Risk Factors. *World J Oncol* **10**, 10-27, doi:10.14740/wjon1166 (2019).

9 Thomas, A. in *global cancer observatory* (2020).

10 Saad, A. M., Turk, T., Al-Husseini, M. J. & Abdel-Rahman, O. Trends in pancreatic adenocarcinoma incidence and mortality in the United States in the last four decades; a SEER-based study. *BMC Cancer* **18**, 688, doi:10.1186/s12885-018-4610-4 (2018).

11 Ilic, M. & Ilic, I. Epidemiology of pancreatic cancer. *World J Gastroenterol* **22**, 9694-9705, doi:10.3748/wjg.v22.i44.9694 (2016).

12 Luchini, C., Capelli, P. & Scarpa, A. Pancreatic Ductal Adenocarcinoma and Its Variants. *Surg Pathol Clin* **9**, 547-560, doi:10.1016/j.path.2016.05.003 (2016).

13 McGuigan, A. *et al.* Pancreatic cancer: A review of clinical diagnosis, epidemiology, treatment and outcomes. *World J Gastroenterol* **24**, 4846-4861, doi:10.3748/wjg.v24.i43.4846 (2018).

14 Keane, M. G., Horsfall, L., Rait, G. & Pereira, S. P. A case-control study comparing the incidence of early symptoms in pancreatic and biliary tract cancer. *BMJ Open* **4**, e005720, doi:10.1136/bmjopen-2014-005720 (2014).

15 Canto, M. I. *et al.* International Cancer of the Pancreas Screening (CAPS) Consortium summit on the management of patients with increased risk for familial pancreatic cancer. *Gut* **62**, 339-347, doi:10.1136/gutjnl-2012-303108 (2013).

16 Vincent, A., Herman, J., Schulick, R., Hruban, R. H. & Goggins, M. Pancreatic cancer. *Lancet* **378**, 607-620, doi:10.1016/s0140-6736(10)62307-0 (2011).

17 Midha, S., Chawla, S. & Garg, P. K. Modifiable and non-modifiable risk factors for pancreatic cancer: A review. *Cancer Lett* **381**, 269-277, doi:10.1016/j.canlet.2016.07.022 (2016).

18 Silverman, D. T. *et al.* Why do Black Americans have a higher risk of pancreatic cancer than White Americans? *Epidemiology* **14**, 45-54, doi:10.1097/00001648-200301000-00013 (2003).

19 Wolpin, B. M. *et al.* Pancreatic cancer risk and ABO blood group alleles: results from the pancreatic cancer cohort consortium. *Cancer Res* **70**, 1015-1023, doi:10.1158/0008-5472.Can-09-2993 (2010).

20 Memba, R. *et al.* The potential role of gut microbiota in pancreatic disease: A systematic review. *Pancreatology* **17**, 867-874, doi:10.1016/j.pan.2017.09.002 (2017).

21 Stevens, R. J., Roddam, A. W. & Beral, V. Pancreatic cancer in type 1 and young-onset diabetes: systematic review and meta-analysis. *Br J Cancer* **96**, 507-509, doi:10.1038/sj.bjc.6603571 (2007).
22 Huxley, R., Ansary-Moghaddam, A., Berrington de Gonzalez, A., Barzi, F. & Woodward, M. Type-II diabetes and pancreatic cancer: a meta-analysis of 36 studies. *Br J Cancer* **92**, 2076-2083, doi:10.1038/sj.bjc.6602619 (2005).
23 Lankisch, P. G., Apte, M. & Banks, P. A. Acute pancreatitis. *Lancet* **386**, 85-96, doi:10.1016/s0140-6736(14)60649-8 (2015).
24 Amundadottir, L. T. Pancreatic Cancer Genetics. *Int J Biol Sci* **12**, 314-325, doi:10.7150/ijbs.15001 (2016).
25 Hruban, R. H., Canto, M. I., Goggins, M., Schulick, R. & Klein, A. P. Update on familial pancreatic cancer. *Adv Surg* **44**, 293-311, doi:10.1016/j.yasu.2010.05.011 (2010).
26 Becker, A. E., Hernandez, Y. G., Frucht, H. & Lucas, A. L. Pancreatic ductal adenocarcinoma: risk factors, screening, and early detection. *World J Gastroenterol* **20**, 11182-11198, doi:10.3748/wjg.v20.i32.11182 (2014).
27 Iodice, S., Gandini, S., Maisonneuve, P. & Lowenfels, A. B. Tobacco and the risk of pancreatic cancer: a review and meta-analysis. *Langenbecks Arch Surg* **393**, 535-545, doi:10.1007/s00423-007-0266-2 (2008).
28 Wang, Y. T., Gou, Y. W., Jin, W. W., Xiao, M. & Fang, H. Y. Association between alcohol intake and the risk of pancreatic cancer: a dose-response meta-analysis of cohort studies. *BMC Cancer* **16**, 212, doi:10.1186/s12885-016-2241-1 (2016).
29 Raimondi, S., Lowenfels, A. B., Morselli-Labate, A. M., Maisonneuve, P. & Pezzilli, R. Pancreatic cancer in chronic pancreatitis; aetiology, incidence, and early detection. *Best Pract Res Clin Gastroenterol* **24**, 349-358, doi:10.1016/j.bpg.2010.02.007 (2010).
30 Bray, F. in *world cancer reaserch fund* (2018).
31 Hruban, R. H. *et al.* Pancreatic intraepithelial neoplasia: a new nomenclature and classification system for pancreatic duct lesions. *Am J Surg Pathol* **25**, 579-586, doi:10.1097/00000478-200105000-00003 (2001).
32 Peters, M. L. B. *et al.* Progression to pancreatic ductal adenocarcinoma from pancreatic intraepithelial neoplasia: Results of a simulation model. *Pancreatology* **18**, 928-934, doi:10.1016/j.pan.2018.07.009 (2018).
33 Mohammed, S., Van Buren, G., 2nd & Fisher, W. E. Pancreatic cancer: advances in treatment. *World J Gastroenterol* **20**, 9354-9360, doi:10.3748/wjg.v20.i28.9354 (2014).
34 Grant, T. J., Hua, K. & Singh, A. Molecular Pathogenesis of Pancreatic Cancer. *Prog Mol Biol Transl Sci* **144**, 241-275, doi:10.1016/bs.pmbts.2016.09.008 (2016).
35 Morton, J. P. *et al.* Mutant p53 drives metastasis and overcomes growth arrest/senescence in pancreatic cancer. *Proceedings of the National Academy of Sciences of the United States of America* **107**, 246-251, doi:10.1073/pnas.0908428107 (2010).
36 Fahrmann, J. F. *et al.* A Plasma-Derived Protein-Metabolite Multiplexed Panel for Early-Stage Pancreatic Cancer. *J Natl Cancer Inst* **111**, 372-379, doi:10.1093/jnci/djy126 (2019).
37 Versteijne, E. *et al.* Meta-analysis comparing upfront surgery with neoadjuvant treatment in patients with resectable or borderline resectable pancreatic cancer. *Br J Surg* **105**, 946-958, doi:10.1002/bjs.10870 (2018).
38 Kluger, M. D. in *uptodate.com* (2020).
39 Tong, H. X. *et al.* Long-term survival following total pancreatectomy and superior mesenteric-portal vein resection for pancreatic ductal adenocarcinoma: A case report. *Oncol Lett* **9**, 318-320, doi:10.3892/ol.2014.2628 (2015).

40 Romano, G. *et al.* Whipple's pancreaticoduodenectomy: Surgical technique and perioperative clinical outcomes in a single center. *Int J Surg* **21 Suppl 1**, S68-71, doi:10.1016/j.ijsu.2015.06.062 (2015).
41 in *Duke Health* (2018).
42 Riviere, D. *et al.* Laparoscopic versus open distal pancreatectomy for pancreatic cancer. *The Cochrane database of systematic reviews* **4**, Cd011391, doi:10.1002/14651858.CD011391.pub2 (2016).
43 Venkat, R. *et al.* Laparoscopic distal pancreatectomy is associated with significantly less overall morbidity compared to the open technique: a systematic review and meta-analysis. *Ann Surg* **255**, 1048-1059, doi:10.1097/SLA.0b013e318251ee09 (2012).
44 Zhang, J., Wu, W. M., You, L. & Zhao, Y. P. Robotic versus open pancreatectomy: a systematic review and meta-analysis. *Ann Surg Oncol* **20**, 1774-1780, doi:10.1245/s10434-012-2823-3 (2013).
45 Mollberg, N. *et al.* Arterial resection during pancreatectomy for pancreatic cancer: a systematic review and meta-analysis. *Ann Surg* **254**, 882-893, doi:10.1097/SLA.0b013e31823ac299 (2011).
46 Springfeld, C. *et al.* Chemotherapy for pancreatic cancer. *Presse Med* **48**, e159-e174, doi:10.1016/j.lpm.2019.02.025 (2019).
47 Neoptolemos, J. P. *et al.* Adjuvant chemotherapy with fluorouracil plus folinic acid vs gemcitabine following pancreatic cancer resection: a randomized controlled trial. *Jama* **304**, 1073-1081, doi:10.1001/jama.2010.1275 (2010).
48 Neoptolemos, J. P. *et al.* Comparison of adjuvant gemcitabine and capecitabine with gemcitabine monotherapy in patients with resected pancreatic cancer (ESPAC-4): a multicentre, open-label, randomised, phase 3 trial. *Lancet* **389**, 1011-1024, doi:10.1016/s0140-6736(16)32409-6 (2017).
49 Ghosn, M. *et al.* Where does chemotherapy stands in the treatment of ampullary carcinoma? A review of literature. *World J Gastrointest Oncol* **8**, 745-750, doi:10.4251/wjgo.v8.i10.745 (2016).
50 Conroy, T. *et al.* FOLFIRINOX or Gemcitabine as Adjuvant Therapy for Pancreatic Cancer. *The New England journal of medicine* **379**, 2395-2406, doi:10.1056/NEJMoa1809775 (2018).
51 Conroy, T. *et al.* FOLFIRINOX versus gemcitabine for metastatic pancreatic cancer. *The New England journal of medicine* **364**, 1817-1825, doi:10.1056/NEJMoa1011923 (2011).
52 Chu, Q. D. *et al.* Virotherapy using a novel chimeric oncolytic adenovirus prolongs survival in a human pancreatic cancer xenograft model. *Surgery* **152**, 441-448, doi:10.1016/j.surg.2012.05.040 (2012).
53 Wang-Gillam, A. *et al.* Nanoliposomal irinotecan with fluorouracil and folinic acid in metastatic pancreatic cancer after previous gemcitabine-based therapy (NAPOLI-1): a global, randomised, open-label, phase 3 trial. *Lancet* **387**, 545-557, doi:10.1016/s0140-6736(15)00986-1 (2016).
54 Lal, S. *et al.* WEE1 inhibition in pancreatic cancer cells is dependent on DNA repair status in a context dependent manner. *Scientific reports* **6**, 33323, doi:10.1038/srep33323 (2016).
55 Golan, T. *et al.* Maintenance Olaparib for Germline BRCA-Mutated Metastatic Pancreatic Cancer. *The New England journal of medicine* **381**, 317-327, doi:10.1056/NEJMoa1903387 (2019).
56 Jackson, S. P. Sensing and repairing DNA double-strand breaks. *Carcinogenesis* **23**, 687-696, doi:10.1093/carcin/23.5.687 (2002).
57 Ohnishi, T., Mori, E. & Takahashi, A. DNA double-strand breaks: their production, recognition, and repair in eukaryotes. *Mutat Res* **669**, 8-12, doi:10.1016/j.mrfmmm.2009.06.010 (2009).
58 Peng, G. & Lin, S. Y. Exploiting the homologous recombination DNA repair network for targeted cancer therapy. *World J Clin Oncol* **2**, 73-79, doi:10.5306/wjco.v2.i2.73 (2011).
59 Buisson, R. *et al.* Cooperation of breast cancer proteins PALB2 and piccolo BRCA2 in stimulating homologous recombination. *Nat Struct Mol Biol* **17**, 1247-1254, doi:10.1038/nsmb.1915 (2010).

60 Sunada, S., Nakanishi, A. & Miki, Y. Crosstalk of DNA double-strand break repair pathways in poly(ADP-ribose) polymerase inhibitor treatment of breast cancer susceptibility gene 1/2-mutated cancer. *Cancer Sci* **109**, 893-899, doi:10.1111/cas.13530 (2018).
61 Thompson, N., Adams, D. J. & Ranzani, M. Synthetic lethality: emerging targets and opportunities in melanoma. *Pigment Cell Melanoma Res* **30**, 183-193, doi:10.1111/pcmr.12573 (2017).
62 Sonnenblick, A., de Azambuja, E., Azim, H. A., Jr. & Piccart, M. An update on PARP inhibitors--moving to the adjuvant setting. *Nat Rev Clin Oncol* **12**, 27-41, doi:10.1038/nrclinonc.2014.163 (2015).
63 Bochum, S., Berger, S. & Martens, U. M. Olaparib. *Recent Results Cancer Res* **211**, 217-233, doi:10.1007/978-3-319-91442-8_15 (2018).
64 Musella, A. *et al.* Rucaparib: An emerging parp inhibitor for treatment of recurrent ovarian cancer. *Cancer Treat Rev* **66**, 7-14, doi:10.1016/j.ctrv.2018.03.004 (2018).
65 Heo, Y. A. & Duggan, S. T. Niraparib: A Review in Ovarian Cancer. *Target Oncol* **13**, 533-539, doi:10.1007/s11523-018-0582-1 (2018).
66 Shirley, M. Rucaparib: A Review in Ovarian Cancer. *Target Oncol* **14**, 237-246, doi:10.1007/s11523-019-00629-5 (2019).
67 Boussios, S. *et al.* Veliparib in ovarian cancer: a new synthetically lethal therapeutic approach. *Invest New Drugs* **38**, 181-193, doi:10.1007/s10637-019-00867-4 (2020).
68 Yin, L. *et al.* PARP inhibitor veliparib and HDAC inhibitor SAHA synergistically co-target the UHRF1/BRCA1 DNA damage repair complex in prostate cancer cells. *J Exp Clin Cancer Res* **37**, 153, doi:10.1186/s13046-018-0810-7 (2018).
69 Litton, J. K. *et al.* Talazoparib in Patients with Advanced Breast Cancer and a Germline BRCA Mutation. *The New England journal of medicine* **379**, 753-763, doi:10.1056/NEJMoa1802905 (2018).
70 Almahli, H. *et al.* Development of novel synthesized phthalazinone-based PARP-1 inhibitors with apoptosis inducing mechanism in lung cancer. *Bioorg Chem* **77**, 443-456, doi:10.1016/j.bioorg.2018.01.034 (2018).
71 Howe, K. *et al.* The zebrafish reference genome sequence and its relationship to the human genome. *Nature* **496**, 498-503, doi:10.1038/nature12111 (2013).
72 Steenbergen, P. J., Bardine, N. & Sharif, F. Kinetics of glucocorticoid exposure in developing zebrafish: A tracer study. *Chemosphere* **183**, 147-155, doi:10.1016/j.chemosphere.2017.05.059 (2017).
73 Cayuela, M. L. *et al.* The Zebrafish as an Emerging Model to Study DNA Damage in Aging, Cancer and Other Diseases. *Front Cell Dev Biol* **6**, 178, doi:10.3389/fcell.2018.00178 (2018).
74 Vierstraete, J. *et al.* Accurate quantification of homologous recombination in zebrafish: brca2 deficiency as a paradigm. *Scientific reports* **7**, 16518, doi:10.1038/s41598-017-16725-3 (2017).
75 Reimers, M. J., La Du, J. K., Periera, C. B., Giovanini, J. & Tanguay, R. L. Ethanol-dependent toxicity in zebrafish is partially attenuated by antioxidants. *Neurotoxicol Teratol* **28**, 497-508, doi:10.1016/j.ntt.2006.05.007 (2006).
76 Hidalgo, M. *et al.* Patient-derived xenograft models: an emerging platform for translational cancer research. *Cancer Discov* **4**, 998-1013, doi:10.1158/2159-8290.Cd-14-0001 (2014).
77 Gaudenzi, G. *et al.* Patient-derived xenograft in zebrafish embryos: a new platform for translational research in neuroendocrine tumors. *Endocrine* **57**, 214-219, doi:10.1007/s12020-016-1048-9 (2017).
78 Veinotte, C. J., Dellaire, G. & Berman, J. N. Hooking the big one: the potential of zebrafish xenotransplantation to reform cancer drug screening in the genomic era. *Dis Model Mech* **7**, 745-754, doi:10.1242/dmm.015784 (2014).

79 London, S. & Volkoff, H. Effects of fasting on the central expression of appetite-regulating and reproductive hormones in wild-type and Casper zebrafish (Danio rerio). *Gen Comp Endocrinol* **282**, 113207, doi:10.1016/j.ygcen.2019.06.011 (2019).
80 Fior, R. *et al.* Single-cell functional and chemosensitive profiling of combinatorial colorectal therapy in zebrafish xenografts. *Proceedings of the National Academy of Sciences of the United States of America* **114**, E8234-e8243, doi:10.1073/pnas.1618389114 (2017).
81 Chen, G. in *StemBook* (Harvard Stem Cell Institute
Copyright: (c) 2012 Guokai Chen., 2008).
82 White, R. M. *et al.* Transparent adult zebrafish as a tool for in vivo transplantation analysis. *Cell Stem Cell* **2**, 183-189, doi:10.1016/j.stem.2007.11.002 (2008).
83 Coelho, G. C. Z. *et al.* Preparation of a fish embryo for micromanipulation: staging of development, removal of the chorion and traceability of PGCs in Prochilodus lineatus. *Int J Dev Biol* **63**, 57-65, doi:10.1387/ijdb.180348gc (2019).
84 Schmelzer, E. *et al.* Response of Human Fetal Liver Progenitor Cell Types to Temperature and pH Stresses In Vitro. *Rejuvenation Res* **21**, 257-269, doi:10.1089/rej.2016.1890 (2018).
85 Sereti, E. *et al.* Patient Derived Xenografts (PDX) for personalized treatment of pancreatic cancer: emerging allies in the war on a devastating cancer? *J Proteomics* **188**, 107-118, doi:10.1016/j.jprot.2018.01.012 (2018).
86 Fong, D., Duceppe, N. & Hoemann, C. D. Mesenchymal stem cell detachment with trace trypsin is superior to EDTA for in vitro chemotaxis and adhesion assays. *Biochem Biophys Res Commun* **484**, 656-661, doi:10.1016/j.bbrc.2017.01.171 (2017).
87 Vlecken, D. H. & Bagowski, C. P. LIMK1 and LIMK2 are important for metastatic behavior and tumor cell-induced angiogenesis of pancreatic cancer cells. *Zebrafish* **6**, 433-439, doi:10.1089/zeb.2009.0602 (2009).
88 Tsuji, K. *et al.* Effects of Different Cell-Detaching Methods on the Viability and Cell Surface Antigen Expression of Synovial Mesenchymal Stem Cells. *Cell Transplant* **26**, 1089-1102, doi:10.3727/096368917x694831 (2017).
89 Nicoli, S. & Presta, M. The zebrafish/tumor xenograft angiogenesis assay. *Nat Protoc* **2**, 2918-2923, doi:10.1038/nprot.2007.412 (2007).
90 Nicoli, S., Ribatti, D., Cotelli, F. & Presta, M. Mammalian tumor xenografts induce neovascularization in zebrafish embryos. *Cancer Res* **67**, 2927-2931, doi:10.1158/0008-5472.Can-06-4268 (2007).
91 Murai, J. Targeting DNA repair and replication stress in the treatment of ovarian cancer. *Int J Clin Oncol* **22**, 619-628, doi:10.1007/s10147-017-1145-7 (2017).
92 Murai, J. *et al.* Stereospecific PARP trapping by BMN 673 and comparison with olaparib and rucaparib. *Mol Cancer Ther* **13**, 433-443, doi:10.1158/1535-7163.Mct-13-0803 (2014).
93 Rodriguez-Mari, A. *et al.* Roles of brca2 (fancd1) in oocyte nuclear architecture, gametogenesis, gonad tumors, and genome stability in zebrafish. *PLoS Genet* **7**, e1001357, doi:10.1371/journal.pgen.1001357 (2011).

10. Addendum

1. H&E protocol

1. Bath 1 toluene 5’ Chemlab
2. Bath2 toluene 5’
3. Bath3 toluene 5’
4. Bath4 isopropanol 2’ Chemlab
5. Bath5 isopropanol 2’
6. Bath6 alcohol 96% 2’ Chemlab
7. Bath7 alcohol 96% 2’
8. Bath29 water 2’
9. Bath19 aqua dest. 1’
10. Bath15 haematox. 15” VWR (Merck)
11. Bath29 lwater 2’
12. Bath16 clarifier I 1’ Thermo scientific (Richard Allan Scientific)
13. Bath29 water 1’
14. Bath17 bluing reagent 1’ Thermo scientific (Richard Allan Scientific)
15. Bath29 water 1’
16. Bath19 aqua dest. 1’
17. Bath18 eosin+phloxine 30” Thermo scientific (Richard Allan Scientific)
18. Bath29 water 2’
19. Bath20 alcohol 96% 2’
20. Bath21 alcohol 96% 2’
21. Bath22 isopropanol 2’
22. Bath8 isopropanol 2’
23. Bath9 toluene 2’
24. Bath23 toluene 2’
25. Bath38 toluene 1’
26. Cover with Mounting Media Thermo scientific (Richard Allan Scientific)

2. Ford protocol

	Time	Temperature
1. Activation	3 min	95°C
2. Denaturation	15 sec	95°C
3. Annealing	10 sec	60°C
4. Elongation	15 sec	72°C
35 cycli (2-4)		
Final	1 min	72°C

3. KAPA2G Robust HotStart ReadyMix Ford

The KAPA2G Robust HotStart ReadyMix Ford contains polymerase, dNTPs, $MgCl_2$ and stabilizers. To prepare the PCR master mix, the ingredients need to be added as stated in table 2.

Table 2: ingredients KAPA2G Robust HotStart ReadyMix Ford

component	10µL reaction
5XKAPA2G Robust HotStart RaedyMix	5µL
2µM Forward Primer	1,25µL
2µM Reverse Primer	1,25µL
Template DNA	2,5µL

4. Capillary electrophoresis

The Fragment Analyzer uses capillary electrophoresis to separate DNA fragments. The wild type *brca2*$^{+/+}$ gene can be separated from the *brca2*$^{-/-}$ mutant as the mutant gene lacks 13pb. The figure below displays the results of the fragment analyzer for a wild type and mutant and *brca2* DNA fragment.